

SORA 3: Stratospheric Organism and Radiation Analyzer

R. B. Masek,¹ T. D. Hill,² D. W. Howard,³ J. Patel,¹ J. Alvarado,¹ C. Amaya,⁴ A. Boggs,¹ C. Bush,⁵ A. Carpy,¹ K. Fleming,⁶ E. Humble,¹ S. Ngiang,⁷ K. Ngo,¹ H. Trong,⁷ A. Vega,⁷ S. George,¹ I. Wilson,⁵ D. Pattison,⁵ P. Gunaratne,⁵ A. L. Renshaw,¹ and O. K. Varghese¹

¹*College of Natural Sciences and Mathematics, Department of Physics, University of Houston, Houston, TX, 77204, USA*

²*Walter Scott Jr. College of Engineering, School of Advanced Materials Discovery, Colorado State University, Fort Collins, CO, 80521*

³*Cullen College of Engineering, Department of Electrical Engineering, University of Houston, Houston, TX, 77204, USA*

⁴*College of Natural Sciences and Mathematics, Department of Computer Science, University of Houston, Houston, TX, 77204, USA*

⁵*College of Natural Sciences and Mathematics, Department of Biology, University of Houston, Houston, TX, 77204, USA*

⁶*Cullen College of Engineering, Department of Chemical and Biomolecular Engineering, University of Houston, Houston, TX, 77204, USA*

⁷*Cullen College of Engineering, Department of Mechanical Engineering, University of Houston, Houston, TX, 77204, USA*

Abstract

The SORA 3 experiment sought to continue the work performed by the previous two SORA iterations. The primary goal of the SORA 3 experiment was to use the foundation that was developed over the previous two years to improve the astrobiology collection mechanism, expand the existing radiation system to account for two Timepix devices, and add a new organic solar cell study. The new payload featured an overhauled astrobiology system which utilized mechanical rotation to sample the stratospheric environment. Using the software developed for the 2018 SORA mission, a FITPix device was added to the payload. The new device allowed the previously used MiniPIX device to be housed inside a mock-up International Space Station (ISS) module which sought to simulate the environment inside the actual ISS. The software was modified to account for the additional Timepix device so that the two devices would simultaneously record data. Lastly, the organic solar cell experiment aimed to expose such cells to the stratosphere and observe the structural degradation and performance change to the cells. Overall, the SORA 3 experiment did not succeed as each experiment had its own difficulties and points of failure. The material of the astrobiology container experienced deformation which prohibited the mechanical arm from spinning, the Timepix devices collected data for several hours but stopped and could not be rebooted due to the dysfunctional astrobiology motor, and the solar cell fabrication lab had issues with material quality during the days leading up to flight. Despite these failures, the design and methodology of the payload provided valuable knowledge and can serve as a stepping stone for future iterations of the SORA experiments.

CONTENTS

1. Mission Objectives and Background	1
1.1. Astrobiology Background	1
1.2. Radiation Background	2
2. SORA 3 Payload Design	3
2.1. Payload Structure	3
2.2. Hardware and Electronics	4
2.2.1. Power Supply	4
2.2.2. Flight Computer	5
2.2.3. DC Stepper Motor	5
2.3. Astrobiology System Design	7
2.4. Radiation System Design	7
2.4.1. Radiation Monitoring	7
2.4.2. Organic Solar Cells	9
2.4.3. In Situ Measurements	11
2.4.4. Active Layer	11
2.4.5. Transport Layers	12
2.4.6. Electrodes	12
2.4.7. Fabrication Ready Lab Search	12
2.4.8. Encapsulation	13
2.4.9. Payload Housing	13
2.5. Telemetry	13
2.5.1. Uplink	13
2.5.2. Downlink	13
3. Methods	14
3.1. Astrobiology Methods	14
3.1.1. Construction and Sanitation	14
3.1.2. Assembly and Transportation	14
3.2. Cosmic Radiation Methods	15
3.3. Organic Solar Cell Methods	17
3.3.1. Fabrication	17
4. Results	18
4.1. Astrobiology Results	19
4.2. Cosmic Radiation Results	19
4.3. Organic Solar Cell Results	19

5. Discussion	21
5.1. Electronics Discussion	22
5.2. Astrobiology Discussion	24
5.3. Radiation Discussion	25
5.3.1. Comsic Radiation	25
5.3.2. Organic Solar Cells	25
6. Conclusion	26
A. Collaboration Demographical Information	27
B. Outreach and Publications	27
C. Internships, Jobs, Recent Graduates, and Graduate School	28
References	30

1. MISSION OBJECTIVES AND BACKGROUND

The Stratospheric Organism and Radiation Analyzer (SORA) 3 is the third generation of a family of experiments. The overarching goal shared by each of the experiments is to collect stratospheric extremophiles and to characterize the radiation environment between the Earth's surface to the HASP float altitude (~ 35 km). SORA 3 had the following scientific objectives:

Primary Scientific Objectives:

1. Capture microorganisms in the upper atmosphere at altitudes of approximately 30 km to 35 km using a method not previously used by the UH HASP team.
2. Study the cosmic and terrestrial radiation to which extremophiles and astronauts are exposed.
3. Observe the performance of organic solar cells in a near-space environment.

Secondary Scientific Objectives:

1. Test the newly developed astrobiology hardware during flight and establish a more reliable method for collecting microbes in extreme environments at high-altitudes.
2. Establish a methodology which allows two or more Medipix devices to be used simultaneously.
3. Study and test our organic solar cell fabrication methods in a highly irradiated environment.

Engineering Objectives:

1. Develop a new astrobiology collection mechanism that is favorable at high altitude.
2. Construct a structure resembling an ISS module as accurately as possible.
3. Analyze radiation data in real time and downlink relevant information.
4. Develop active layers for organic solar cells which can withstand the stratospheric environment.

1.1. Astrobiology Background

Extremophiles are microorganisms that thrive in physically and/or chemically extreme conditions, which are detrimental to most of life on Earth. These organisms and microbes have been found everywhere, from deep underwater volcano vents to buried ice lakes in Antarctica [1].

Fungi and bacterial spores have also been found in the stratosphere. Today, the most common altitudes for organism and microbe collection in the atmosphere are in the range of approximately 10 km to 20 km above Earth's surface. As illustrated in Table I, very little data exists on microbiological samples captured in the stratosphere [1]. Conditions at altitudes of 30 km to 40 km are extreme in temperature, pressure and radiation exposure. Arguably, each successful collection expedition, of at least 30 km into the upper atmosphere, provides information that can be useful in determining what life forms can exist inside and outside of Earth's biosphere. Additionally, RNA analysis of the organisms and microbes can provide useful insight pertaining to their ability to survive in an environment with elevated levels of radiation.

Our experiment focused on designing a more energy efficient compact collection apparatus that refining our sanitation procedures for preflight assembly, post flight disassembly, and RNA sequencing preparation. We also tested effectiveness of rotating filters to stationary ones. The samples we have collected play

an important role in expanding our knowledge about Earth’s biosphere. Future studies could produce meaningful contributions to the fields of gene therapy, RNA interface, and cosmic shielding; and provide valuable insight about how life can be distributed on Earth, and ultimately, through outer-space.

Our experiment was an attempt to further develop our technique for capturing microorganisms in the upper atmosphere, as demonstrated during our 2017 [2] flight which was inspired by the LSU HASP 2011, 2012, 2013 flights [3] and from research by D.R. Canales [4]. The use of a rotating arm mechanism to sample the air for microorganisms through the use of fluoropore membrane filters, proved to be a challenging feat met with difficulties. The samples are an important part to expanding our understanding of Earth’s biosphere. Further studies could provide more insight on how life can be distributed on Earth, and ultimately, through outer-space.

TABLE I. History of Microbiological Sampling of the stratosphere [2].

Date	Altitude (km)	Sample Method	Biology Measured	Volume
1936	11 - 12	Balloon	5 Bacillus sp., 1 Penicillium sp., 1 Macrosporium sp., 2 Aspergillus sp.	<i>Unknown</i>
1978	48 - 77	Meteorological rocket	Mycobacterium sp., Mircococcus sp.	<i>Unknown</i>
2003	30 - 41	Balloon, liquid neon cryopump	Isolated <i>S. pastuerii</i> , <i>B. simplex</i> , the fungus, <i>Egnydontium album</i>	57
2004	20	Airplane, impactor surfaces	Bacillus luciferins, Bacillus sphaericus	<i>Unknown</i>
2006	19 - 41	Balloon, liquid neon cryopump	7 cells L-1 (counting clumps), Bacillus sp., Staphylococcus sp., Engyodontium sp.	19 – 81
2007	20	Airplane, impactor surfaces	Micrococci, Microbacteria, Staphylococcus sp., Brevibacterium sp.	<i>Unknown</i>
2010	20	Airplane, impactor surfaces	Isolated Bacillus sp.	<i>Unknown</i>
2017	32	Balloon, liquid medium w/ vacuum pump	Multiple findings [2]	<i>Unknown</i>
2018	32	Balloon, liquid medium w/ vacuum pump	Inconclusive [5]	<i>Unknown</i>
2019	32	Balloon, Rotating Passive Design	Inconclusive	<i>Unknown</i>

1.2. Radiation Background

Primary cosmic rays is an umbrella term that describes a group of high-energy, charged particles. These particles are typically partially or fully ionized atoms with the major constituents being hydrogen and helium nuclei respectively making up about 89% and 10% of the spectrum [6] [7]. When a primary particle collides with a molecule in the atmosphere, secondary particles are produced which then collide with molecules causing a cascade of particles known as an air shower [8]. The products of air showers are electrons, muons, neutrinos, electromagnetic waves, and various other particles which can be detected on the Earth’s surface. By measuring these particles and gathering information about the air shower, the type, energy, and direction of the primary particle can be extrapolated. The initial energy of the primary particle determines the penetration depth of the air shower, however, most air showers have a maximum secondary particle density at an altitude within the range of 15 km to 20 km known as the Regener-Pfotzer Maximum [9] [10]. The altitude and strength of this maximum is dependent on several factors such as the solar cycles, time of year, and latitude and longitude. The cosmic ray flux has contributions from the Sun (solar cosmic rays), the galaxy, and outside the galaxy [8]. Cosmic rays which have galactic and extra-galactic origins are known as galactic cosmic rays (GCRs) and are responsible for the majority of the observed particle flux in the atmosphere. Interestingly, the GCR flux modulates inversely with the solar cycle in events that are known as a Forbush Decrease [10] [11] [12]. NASA reports that astronauts aboard the International Space Station

(ISS) receive about double the radiation dose during a solar minimum than they do during a solar maximum [13]. Furthermore, recent behavior exhibited by the Sun has resulted in the highest observed GCR flux since the dawn of the space age [14], causing concern regarding the safety of humans in space.

Naturally, this unexpected behavior from the Sun calls for careful monitoring of humans in space and the skies. Commercial airplanes fly in a portion of the atmosphere in which the radiation flux is higher, resulting in increased radiation exposure for frequent fliers and airline crew compared to those who fly at most a couple times a year. This is a huge motivation for the radiation monitoring portion of our experiment with which we aim to develop a nonintrusive, inexpensive radiation dosimeter. SORA uses Medipix-based [15] devices to record data. The SORA 3 experiment used two such devices: one is the MiniPIX [16], and the other is a FITPix [17]. These devices have a USB interface and are capable of detecting charged particles by use of a Timepix sensor [18]. The Timepix sensor is made up of an array of 256 by 256 pixels with a total surface area of 198.25 mm². Each pixel in the array is its own sensor with its own set of readout electronics. The details of the chip construction is given by Jakubek in Ref. [19].

The previous two SORA experiments possessed solely the MiniPIX sensor in very similar configurations each time. SORA 3 expanded upon this construction with the addition of the FITPix in attempt to accurately model the environment inside the ISS with a small container. Ideally, this model would be effective, enabling data collection that is comparable to that data collected aboard the ISS. If successful, this would prove the effectiveness of relatively simple constructions to model rather complex or exotic environments. Furthermore, this would urge more accurate modelling of environments in which human lives are at great risk. Lastly, this would push the boundary of using Timepix devices as radiation dosimeters.

For the third University of Houston's (UH) third mission with the HASP program, we elected to include a new research project along with our prior two projects. Following the success of our previous two missions [2] [5] using the semiconductor based MiniPIX radiation detector we decided to investigate the performance of solar cells in the stratosphere. For space applications [20], solar panels are judged on their deliverable power divided by their weight, known as specific power [W/kg], and their deliverable power divided by the stowed packing volume, known as the stowed packing efficiency [W/V]. When considering these two critical factors we determined that organic photovoltaic (OPV) materials have the potential to maximize both values[21], contingent on their successful operation in the near space environment. This decision is based on the fact that the weight of OPV modules is nearly completely determined by the weight of the substrate on which it is processed, and if that substrate is a flexible foil it allows the stowed packing volume to be cut down by multiple orders of magnitude along with the weight when compared to traditional Gallium Arsenide (GaAs) or Silicon (Si) panels. One of the drawbacks of OPV has been lower efficiencies when compared to other PV technologies, however we feel this is not a disadvantage for the satellite and LEO spacecraft industry where energy demands are not as great.

Our group ran into delays finding a functioning lab space and in achieving efficiencies >3%. Originally we had planned on analyzing both polymeric OPVs as well as perovskite based hybrid-OPV modules, but focused primarily on the polymer OPV modules with the understanding that perovskite cells are fabricated in a similar way[22] and have been achieving much higher conversion efficiencies than the polymer modules. For this reason, we consider this year's mission to be a proof of concept. A circuit was developed by the electronics team to analyze each cell during flight, and the radiation team was able to fabricate OPV modules in a UH lab. We hope to continue our investigation in the future by considering modules with greater conversion efficiencies or more complex architectures (such as tandem cells) which require more complex fabrications.

2. SORA 3 PAYLOAD DESIGN

2.1. Payload Structure

One major design goal of the SORA 3 mission was to make the overall layout of the payload more modular such that each subsystem was not dependent on the presence of other subsystems. A rendering of the design can be seen in Figure 1, and an overview of the electronics system can be seen in Figure 2. This was a major

change from previous missions in which systems and components were not organized leading to massive disorganization across the payload. The modular structure not only organized the systems, but it made it such that the now independent systems could function in the absence of other systems, thus leading to continued functionality of the payload in the event of an in situ failure.

The modular organization was accomplished by compartmentalizing each subsystem into its own structure. The payload was broken up into four main substructures: the astrobiology system, the two radiation containers, and the electronics box. The electronics box served to join all systems together, and the other subsystems could easily be added or removed to the electronics box. The electronics box was made from an easy-to-form PVC/acrylic, which has been proven to work well for previous missions as it can withstand the extreme environment of the stratosphere and is easily machinable. The construction and materials of the astrobiology box and the radiation containers are discussed in their respective sections.

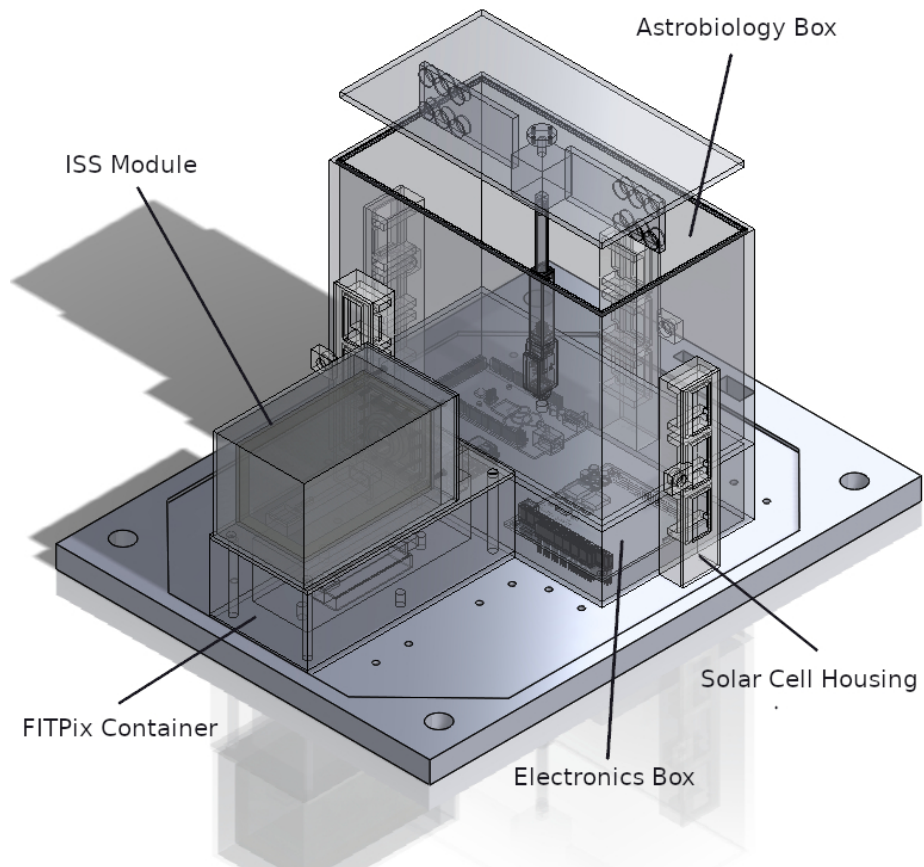


FIG. 1. A final 3D rendering of the payload.

2.2. Hardware and Electronics

2.2.1. Power Supply

The SORA 3 payload used a WinSystems PPM-DC-ATX-P power supply unit (PSU). This unit has several properties that are very attractive for applications such a high altitude balloon flight. To power the flight computer and hardware we received the 30 V DC supply from HASP which we fed to our PSU that supplied

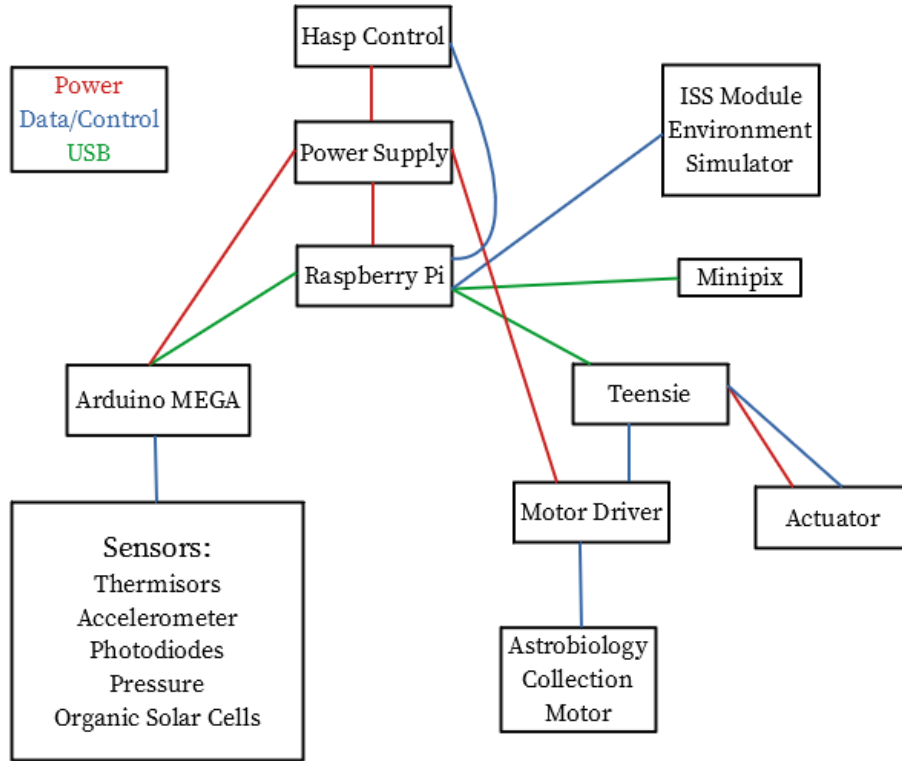


FIG. 2. An overview of the payload’s electronics configuration.

our flight computer and sensor electronics with +5 V, and our current-to-voltage operational amplifiers with +12 V and −12 V. The pins used for the SORA 3 payload are marked in Figure 3. It has an input range of 10 V to 50 V, so the PSU is capable of withstanding any variation in voltage caused by HASP’s depleting batteries. Additionally, this PSU is rated to operate from −40 °C to 85 °C, which is within the environmental variation of temperatures in the stratosphere. More technical details can be found on its datasheet at Ref. [28].

2.2.2. Flight Computer

A Raspberry Pi was chosen as the main component of the flight computer as we needed a platform that was capable of storing an SQL database for the large volume of data we had planned to catalog from the solar cells. An SQL database was found to be necessary due to the serial down-link limit imposed by HASP. We also opted to utilize an Arduino MEGA in order to control the majority of the sensors such as the thermistors for temperature readings, multiple photodiodes for capturing light intensity at the solar cells, a pressure sensor for monitoring altitude, and the array of current-to-voltage converters for characterizing the solar cells. Additionally, the Arduino MEGA sent control signals to an Arduino Nano, a very small footprint microcontroller, which controlled an actuator and a DC stepper motor that were required to operate the mechanical system to facilitate the Astrobiology experiment.

2.2.3. DC Stepper Motor

The AccelStepper Arduino Library developed by AirSpayce [29] was integral to the functionality of our motor. In the initial stages of programming the astrobiology robotic components, issues arose when we

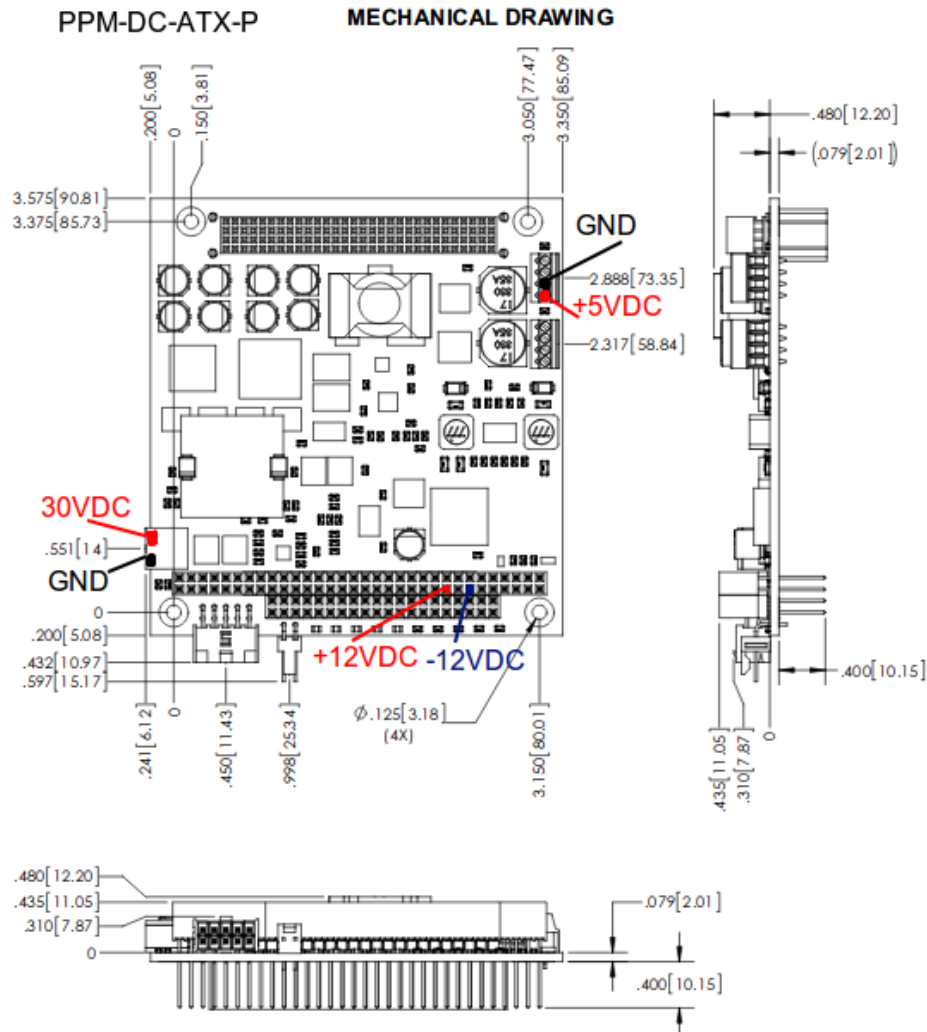


FIG. 3. A detailed schematic of the PSU taken from its datasheet. The pins that were used for the SORA 3 payload are marked on the diagram.

discovered the stepper motor would miscount the number of steps it had taken while accelerating, due to the fact that we had programmed it to jump from a velocity of zero to a high velocity without any initial acceleration, resulting steps being missed in the hardware of the motor and therefore an overshoot on the counted steps versus how many the motor actually took. This was problematic because our motor needed to be returned to a specific location to be retracted into the box, due to our rectangular design. If the motor was off the mark, the payload would be damaged when the lid retracted. In order to accomplish this goal, we needed to specify in our code exactly how many steps to take to turn back to this position.

Setting the acceleration of the motor within the regular stepper motor library was not an option with the initial setup. While there is a function that accomplished this, it blocks the rest of the code from running until the motor has finished its turn. This was not ideal because it meant that our sensor network would be unable to collect data during the time the motor took to spin. The AccelStepper library solved this issue. Based on speed profiles for these types of motors developed by David Austin in "Generate stepper-motor speed profiles in real time", the AccelStepper library allows the appropriate speed to be calculated in real-time, preventing the hang up in the code.

We chose a stepper motor as the motor for our astrobiology collection system due to its ability to rotate 360° degrees continuously. We rejected a simpler servo motor for this reason - most only have the ability to turn 180° and then return to their original position. To accomplish our goal of continuous 360° rotation,

stepper motors were lightweight, inexpensive, and dependable enough to accomplish this task effectively. We chose the NEMA 14 model due to its ability to provide the correct amount of torque needed for our project, while also being able to support the appropriate amount of weight. A DRV8834 motor driver was used to control the voltage supplied to the motor, which made it possible to easily control to torque supplied by the motor. The motor circuit is shown in Figure 4.

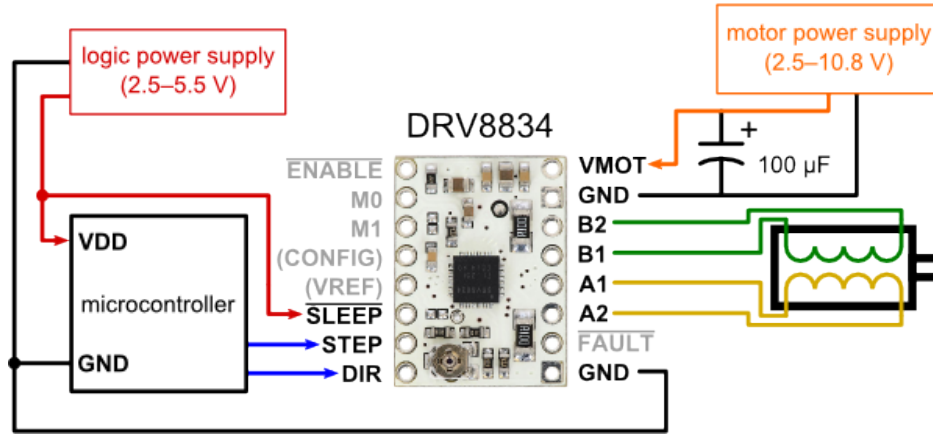


FIG. 4. Circuit showing the stepper motor with its driver. The motor power supply was a direct connection to the PSU, and the logic power supply was provided by the Arduino Nano.

2.3. Astrobiology System Design

The collection assembly was designed as a single mechanized enclosure as shown in the rendering in Figure 5 and the photograph shown in Figure 6. The goal was to make this system fully autonomous with the use of a pressure sensor so that the arm would deploy once the balloon reached float altitude. The rotating arm is raised out of the collection container and begins rotating once the payload reached float attitude. The raising of the rotating arms was done by a L-12 50 mm linear servo motor and the rotation of the filter arm was provided by the rotational motor mounted onto the filter arm. The lid on the top of the linear servo sealed the clean box during ascent and descent. The Fluropore Membrane filters were mounted on the ends of the rotating arm. The arms were set to spin at 80 RPM for the duration of float conditions. In theory, the sampled volume is the cross-sectional area of each filter multiplied by the distance the payload traveled, resulting in a far greater sampled volume than the 0.03 liters per minute sampling of the pumps from the 2018 flight. When the payload began its descent from float conditions, the rotating arm would return to its home position and the linear actuator would retract the rotating mechanism back into the clean box. The Fluropore filters on the rotation arm were compared with those mounted on the linear servo as shown in the figure below. Background samples were taken using the same Fluropore membrane filters; these filters sampled the various places the payload was in, such as the UH lab room, the clean room used for sterilization, and the Fort Sumner launch site. This is done to take the possibility of contamination into consideration during the post-flight filter analysis.

2.4. Radiation System Design

2.4.1. Radiation Monitoring

The radiation monitoring system consists of the two Timepix devices. Each device was placed in separate structures in order to compare the recorded data between devices and to data from previous flights, allowing

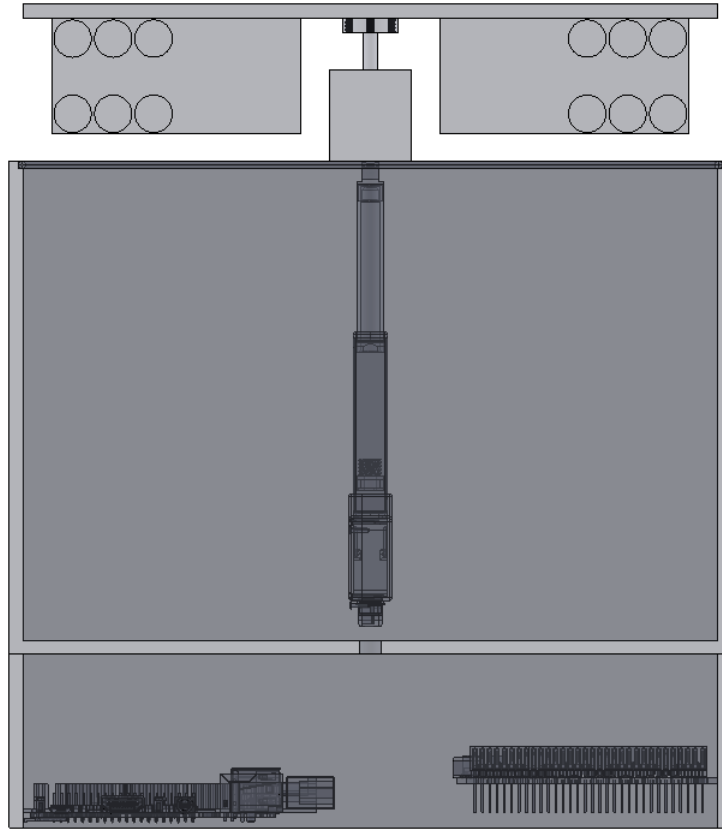


FIG. 5. Side view of the deployed astrobiology system mounted on top of the electronics box. The circles just beneath the lid mark the position and approximate size of the Fluoropore filters.

us to determine effectiveness of the constructed ISS container. The FITPix was placed within a container exactly resembling the contained used for the previous two SORA experiments and acted as the control during the 2019 mission. The MiniPIX was placed inside the mock-up ISS module for two primary reasons. The first being that it would allow a direct comparison between the 2019 data and the data from the previous two SORA missions, since the previous missions used the exact same MiniPIX in the exact same configuration. The second reason was to protect the FITPix. The FITPix used in the SORA 3 mission was a borrowed device, and placing this borrowed device in the new, untested ISS module was deemed inappropriate.

The work of the first two SORA experiments established a strong foundation for the radiation dosimetry portion of the experiment. The software used to control the devices was an extension of the previous year's software with the key difference being that this year's software could accommodate two Timepix devices rather than one. The flight computer had a main thread in which controlled and monitored the entire payload, and new, separate threads would be created to gather the Timepix data so that the sensors and the uplink/downlink connection could be maintained while gathering Timepix data. Once the Timepix data was collected, it would be analyzed in real-time and the particle counts and dose would be sent as part of the downlinked data packet.

The primary structure of the FITPix container was 3D printed using ABS plastic, which is consistent with previous missions. The choice to use 3D printed material is backed by the need to minimize parts needed to construct the container. By minimizing the parts, specifically metal parts, the interactions between the primary particles and the material of the structure are minimized. Ideally, the device would be directly exposed to the atmosphere, but the container is needed to protect the device during landing. There was no concern of the plastic structure becoming compromised since this material has been tested during previous flights and a large heatsink was used to keep the device cool. Shown in Figure 7, two aluminum blocks are

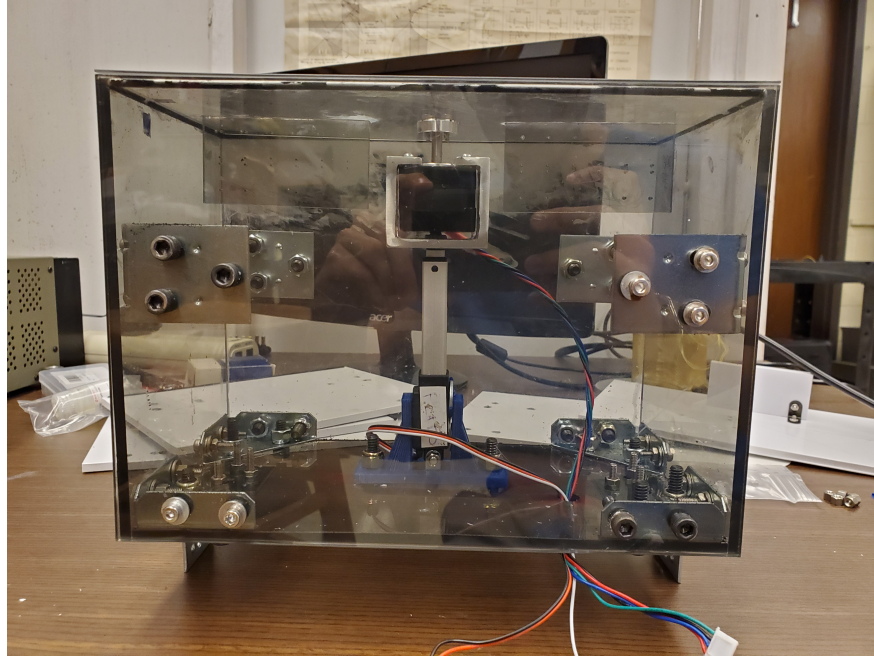


FIG. 6. Photograph of the astrobiology system prior to being sanitized and painted.

used as heatsinks. The device was secured to the smaller block with thermal paste, and the smaller block was secured to the larger piece with thermal paste.

As previously mentioned, the MiniPIX was placed within the mock-up ISS module. The module was constructed using the materials and material proportions given by Ref. [30]. The description of the module layers can be seen in Figure 8. Aluminum 2219-T87 is aircraft grade material, is very expensive (on the order of several thousand dollars), and can only be ordered in bulk. Due to monetary constraints, it was replaced with aluminum 6061-T6, but the dimensions were kept the same. The inner-most (atmosphere-containing) aluminum structure was constructed by cutting sheets for each face of the box then welding the pieces together to form the box. The front face of the box was left open to allow access to the inside of the structure. In order to simulate the ISS environment as closely as possible, the module was to be pressurized at one atmosphere. This was to be accomplished by sealing gaps in the structure with a vacuum epoxy once the entire system was assembled. To measure pressure and temperature inside the module, a sensor was placed inside with wires fed through the layers and sealed with epoxy. Unfortunately, the Nextel layer did not fly due to the long lead time and not receiving the material in time. This almost certainly had an impact in the results of the ISS module experiment.

2.4.2. Organic Solar Cells

The radiation group felt it would be most productive and insightful to be able to fabricate our own cells for launch, as opposed to outsourcing the work to another institution/graduate students or purchasing pre-made cells. With this decision came the reality of learning and understand the functionality behind each layer in the PV stack. The work done by the radiation group over the course of the SORA 3 mission can be divided into three main phases:

1. Materials research/Lab search
2. Device fabrication/encapsulation
3. Launch/post-launch analyses

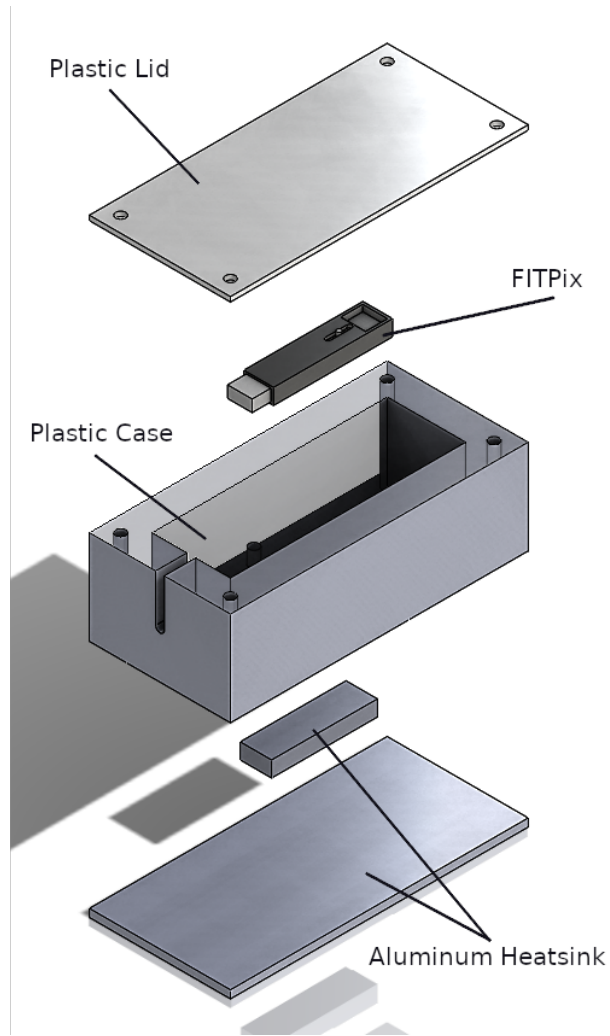


FIG. 7. Exploded view of the FITPix case assembly.

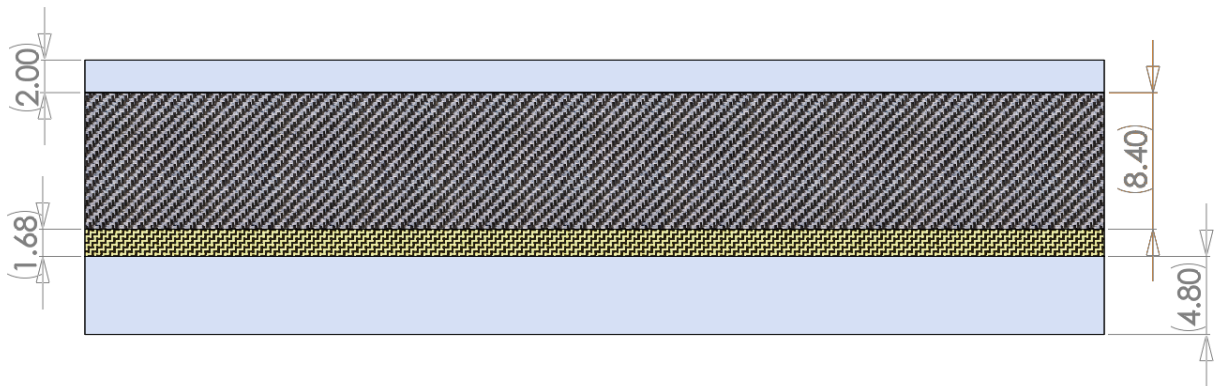


FIG. 8. Layers and thicknesses of the materials that will be used to construct the ISS module. From top to bottom: aluminum 6061-T6, six layers of Nextel AF62, six layers of Kevlar fabric, and aluminum 2219-T87. The atmosphere is contained by the 4.8 mm layer of aluminum. All dimensions are in mm.

We continued to recruit new members while our team started reviewing literature on the fabrication and operation of OPV. Solar cells stacks are categorized by the order in which layers are deposited, either a normal or inverted geometry. The so-called normal geometry consists of a transparent conductive oxide (TCO) for the high work function negative electrode, a hole transporting layer (HTL), active layer, electron transport layer (ETL), and low work function positive electrode (typically a metal). The HTL and ETL work to create an electric field across the active layer to draw out free charges, which are then collected at each electrode. The inverted geometry is characterized by a high work-function, negative top electrode and a hole blocking layer (HBL) atop the positive TCO electrode. Our group adopted the inverted geometry for greater stability of high work function metals.[25]

2.4.3. In Situ Measurements

In order to emulate lab results of solar cell characterization as best as possible in a near-space environment, a current-to-voltage converter circuit was constructed. A digital potentiometer, MPC4131, was used to apply a bias voltage across a solar cell which would produce a current in the micro-Amp range. A combination of two LM2904 operational amplifiers were required to capture both positive and negative current readings which were read as analog values by the Arduino MEGA. The circuit diagram can be seen in Figure 9.

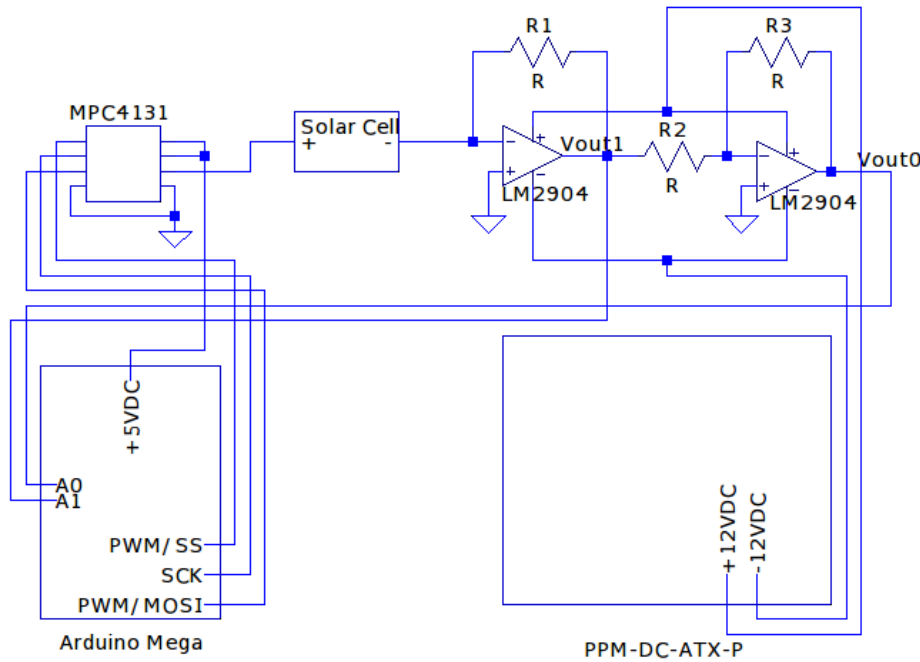


FIG. 9. Circuit diagram of the current-reading circuit constructed for the solar cells.

2.4.4. Active Layer

The greatest consideration is given to the selection of the active layer. The active layer serves the purpose of converting photons (electromagnetic waves) in electrons (useful work)[26]. This happens as the small molecules or conjugated polymers absorb photons with energy greater than their band gap, defined as the difference between the highest occupied molecular level (HOMO) and the lowest unoccupied molecular level (LUMO); in essence the valence and conduction bands of any semiconductor. When photons are absorbed,

electrons are excited from the HOMO to the LUMO band in what is known as the donor. Unlike crystalline semiconductors where charge separation occurs instantly, in organic photoactive materials the electrons remain bound to the left over positive charge, known as the hole, due to Coulombic attraction. This bound electron-hole pair is known as the exciton. The acceptor material will have a LUMO band which is lower in energy than the donor's, causing band bending at the interface and allowing the electron to be separated from the exciton state. Excitons and free charges both have low mobility and short lifetimes within organic materials, thus low diffusion lengths. This means that interfacial domains must be within the nanometer range in order to effectively separate the free charges. This problem has been addressed through the introduction of the bulk heterojunction (BHJ) active layer in which the acceptor and donor molecules are mixed into a single active solution prior to thin film fabrication, resulting in much greater interfacial surface area. An ideal organic active layer would maximize the interfacial surface area while optimizing layer and device thickness for light absorption, exciton diffusion, and charge collection.

In our search we identified many candidate materials for the acceptor and donor molecules but ultimately decided it would be best to focus on the most widely researched BHJ pair of the semi-crystalline polymer Poly(3-hexylthiophene-2,5-diyl) (P3HT) as our donor and the fullerene derivative [6,6]-Phenyl C61 butyric acid methyl ester (PCBM) as our acceptor.

2.4.5. *Transport Layers*

With the selection of the active layer and the knowledge of the inverted geometry stack, every other layer follows naturally. For the HBL we selected a sol-gel titania (TiO_2)^[27]. Fluorine doped tin oxide (FTO) was selected for the TCO opposed to indium doped tin oxide (ITO) due to the high temperatures required for annealing of sol-gel titania HBL. The purpose of annealing the titania solution after film application is to change from the amorphous to the anatase phase. The copolymer Poly(3,4-ethylenedioxythiophene)-poly(styrenesulfonate) (PEDOT:PSS) is most commonly used as a transport layer along with the P3HT:PCBM BHJs and was thus chosen as our EBL.

2.4.6. *Electrodes*

Platinum was selected as our high work function electrode due to availability. The difference between the work functions of platinum and FTO creating the field which causes carrier drift once charges are separated at the P3HT:PCBM interface. With these selections, our completed stack becomes glass/FTO/ TiO_2 /P3HT:PCBM/PEDOT:PSS/Pt.

2.4.7. *Fabrication Ready Lab Search*

One of the greater challenges at the beginning of our mission was acquiring access to a lab with the proper equipment to fabricate the devices ourselves. This search proved difficult due to a combination of a lack of experienced technicians to teach our group the fabrication techniques needed for OPV, a majority of labs only had a portion of the equipment needed in order to fabricate a complete device stack, and the limited budget available to our group for acquisition of materials and for equipment usage. Eventually we were lucky enough to receive permission from Dr. Oommen Varghese to use the equipment and materials within the Nanomaterials and Devices Laboratory where graduate student Lilly Schaffer and Maggie Paulose were both gracious enough to teach our group thin film fabrication techniques and provide insight into the working principles behind OPV. With all materials and equipment secured, the radiation team proceeded into the fabrication phase.

2.4.8. Encapsulation

Due to rapid degradation of organic semiconductors upon contact with moisture or oxygen, encapsulation of organic photovoltaics is essential to maintain longterm stability, especially in the harsh stratospheric environment. We decided to use a glass sandwich secured by epoxy. Once cells were completely fabricated, silver epoxy was used to connect copper wiring onto each metal contact. A new plate of glass was set on top and UV curable epoxy was set around the edge to create a seal.

2.4.9. Payload Housing

To secure and protect each cell during flight we used 3D printed Acrylonitrile Butadiene Styrene (ABS). This provided us the flexibility to redesign an manufacturer secure housing for cells which ended up having various dimensions due to unpredictable manufacturing processes. Cells were set into a recessed cavity with a securing plate set on top with windows to allow light collection for each cell. Between each pair of cells was a smaller cavity for a photodiode to determine the intensity of light on each cell. The housings were screwed near the center on each side of the payload, for a total of four housings and eight cells. The copper wiring from each cell was then soldered to the JV circuit housed below the ISS module.

2.5. Telemetry

2.5.1. Uplink

SORA 3 utilized the three uplink commands shown in Table II. The purpose of the chosen commands was

TABLE II. Uplink commands for the SORA 3 mission.

Command	Command Byte 1	Command Byte 2
Activate astrobiology system	0x11	0x12
Deactivate astrobiology system	0x21	0x22
Reboot SOCRATES	0x31	0x32

to provide broad control over payload systems that would be able to resolve any issues that would crop up during flight. The command to reboot SOCRATES would absolve any issues with the sensor data collection, and the astrobiology system could be manually rebooted by executing the other two commands. If there were any issues with the flight computer (e.g. downlink connection was lost), the HASP power cycle command would be used since an issue with the flight computer would inherently halt all payload operations.

2.5.2. Downlink

The data downlink consisted of all sensor data. The structure of the data packets was as follows:

packet-num, rpi-temp, timepix1-temp, timepix1-dose, timepix1-counts, timepix2-temp, timepix2-dose, timepix2-counts, ambient-pressure, iss-pressure, iss-temp, cell1-temp, cell2-temp, cell3-temp, cell4-temp, cell5-temp, cell6-temp, cell7-temp, cell8-temp, photodiode1, photodiode2, photodiode3, photodiode4, timestamp.

Listing 1 shows an example of some downlink packets received during flight.

Listing 1. Sample of downlinked data packets. The line breaks within each packet was not present in the actual data and are shown here to clearly show the packet.

```
...
1290,34.3,57.6,0.0,0,57.6,0.0,0,-6.20,0.00,0.00,-2.89,16.32,16.09,27.17,
27.80,25.44,-1.81,-0.40,691.00,1023.00,1023.00,78.00,2019-09-05-13:50:18

1291,34.3,57.6,0.3247,2,57.6,0.0652,3,-6.00,0.00,0.00,-2.53,16.22,16.13,
27.26,27.98,25.42,-2.03,-0.42,695.00,1023.00,1023.00,78.00,2019-09-05-13:50:20

1292,35.9,57.6,1.223,5,57.6,0.0420,2,-6.00,0.00,0.00,-2.86,16.09,16.04,
27.15,27.78,25.48,-1.76,-0.13,706.00,1023.00,1023.00,78.00,2019-09-05-13:50:21

1293,34.9,57.6,0.5517,4,57.6,0.0086,1,-6.40,0.00,0.00,-2.92,16.17,16.19,
27.24,27.91,25.55,-1.81,-0.42,712.00,1023.00,1023.00,78.00,2019-09-05-13:50:22
...
```

3. METHODS

3.1. Astrobiology Methods

3.1.1. Construction and Sanitation

The parts were designed in CAD and machined at the University of Houston College of Natural Sciences and Mathematics Workshop. The material used to construct the pieces was a semi-transparent, polycarbonate material with high hardness rating and can withstand a wide temperature range without significant deformation. The clean box itself, including the lid, was constructed using six plates of material with very tight tolerances.

The sterilization procedure was a multistep process requiring different methods for various parts of the collection system. The collection box, control boxes, and various tools for assembly were placed in bags and run through an autoclave, which is a high pressure and high temperature oven designed to sterilize items in biology labs. It was necessary to perform this procedure without the motors or filters installed, as they would be damaged by the conditions of the autoclave. The filters were sterilized by placing them in a clean box and exposing them to UV light for 30 minutes on each side. Once this was done, the boxes and tools were removed from the autoclave and placed in the clean box for assembly, after thoroughly wiping down the bags they were autoclaved in with a 70% ethanol solution. Every individual who placed their hands in the clean box wore nitrile gloves, and rinsed their hands with the ethanol solution each time they entered the clean box. The collection system was then assembled, with everything that could not be autoclaved or placed under UV light—the motors, epoxy, etc.—being thoroughly wiped down with the ethanol solution before being placed in the clean box. Once assembly was complete, the control boxes and the collection box were sealed, ensuring that the interiors remained sterile until deployment and analysis.

Extensive sanitation procedure was carried out before assembly to eliminate any possible sources of contaminating bacteria. The entire collection structure, except for the L-12 linear servo, the stepper motor, and the Fluropore membrane filters, along with any tools used for construction were thermally sterilized in an autoclave at 120 °C for 50 minutes. Then, the servo and motor was wiped down with 70% ethanol solution, and the Fluropore filters were exposed to intense UV light for several hours before assembly.

3.1.2. Assembly and Transportation

The assembly process was performed within a SterilGARD e3 Class II Biological Safety Cabinet. Every individual involved in assembly was garbed in a lab coat, goggles, hair net and latex gloves after thoroughly

washing their hands in a 70% ethanol solution. The filters were threaded onto the wings, and the collection mechanism consisting of the servos and the mechanical arms were installed in the clean box. Rubber lining was placed along the edges where the boxes come into contact with the lid and secured in place with vacuum epoxy. In addition, the screws of the box, as well as any gaps between the plates, were also covered with epoxy to create an airtight seal.

After the assembly process, a signal was sent to the motor to close the lid and seal off the clean box to prepare for transportation. After the collection module was integrated into the rest of the payload, the entire payload will be placed in an autoclave bag to transport to the flight site.

3.2. Cosmic Radiation Methods

The MiniPIX has a built-in temperature sensor that can report the temperature of the device, so this function was used to monitor its temperature. Unfortunately the FITPix does not possess this functionality, but considering the container which housed the FITPix has been tested in previous flights, there was no worry of the FITPix overheating.

The Timepix sensors output data in a human-readable, array-like format that directly corresponds to the pixel array of the sensor. The sensor collects data in a manner similar to that of an optical camera. A shutter time is a parameter defined by the user, and the sensor will collect data for the entire duration of the shutter time. Once the time has lapsed, the sensor packages the data into a data frame and is sent to the storage of the computer. The length of the shutter time must be carefully chosen, and the time for the SORA 3 mission was approximately one second for both devices. Too short of a length will result in many empty data frames that wastes storage space, but too long of a length will result in data frames which are unreadable since the particle tracks in the frame will intersect and be indistinguishable from one another. Each pixel in the 256 by 256 sensor array has one corresponding energy value per frame, so this array can be used to reconstruct the data frame. The energy threshold is another user-defined parameter that determines the minimum energy which can be detected by the sensor. The primary purpose of the energy threshold is to filter out extraneous whitenoise from the environment. An example of a data frame can be seen in Figure 10. A separate file contains the metadata for each data frame, and contained within the metadata is information such as the energy threshold and the timestamp.

Using the techniques detailed by Jakubek et. al. [31], the radiation dose deposited in the sensor by a particle can be calculated using the following equation

$$D_{Si} = \frac{E}{M_d},$$

where E is the total energy that a particle deposited into the sensor and M_d is the mass of the sensor. It is important to note that this dose value is not the same as dose deposited in human flesh, which is referred to as dose equivalent. Conventional calculations for dose equivalent in tissue requires use of Monte Carlo simulations to calculate a conversion factor [32] and is outside the SORA missions' scope of study. Calculating the total energy of a particle requires the use of a clustering algorithm. The clustering algorithm analyzes the raw matrix output from the Timepix sensor and groups the pixels with non-zero energy into clusters, or tracks. The total energy of the cluster, E , is the sum of all pixel energies in the cluster.

Another property of interest from the Timepix data is the linear energy transfer (LET), which provides a standard with which all particle clusters can be examined independent of the particle's incident angle. To calculate the LET in the silicon sensor, the following relation is used

$$LET_{Si} = \frac{E}{L},$$

where E is the same energy value used in the D_{Si} calculation, and L is the length of the track in the detector in three dimensions. The clustering algorithm uses a typical flood-fill technique to group touching pixels with non-zero energy. A minimum-area bounding box is then constructed around the cluster with a linear least square fit line which intersects the bounding box, and the projected track length L_p is taken to be the length of the linear least square fit line. A visual example of the bounding box and the linear least square

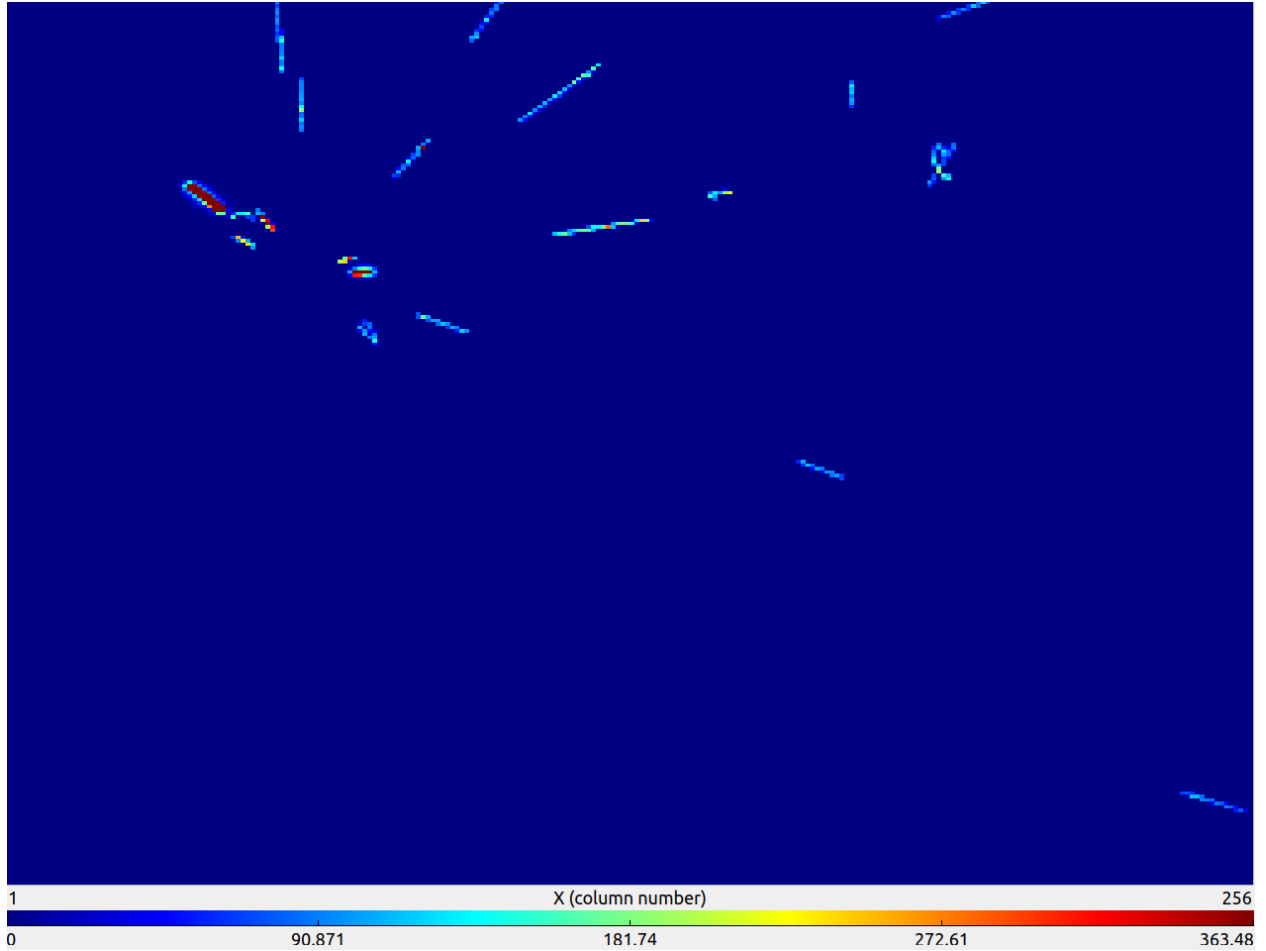


FIG. 10. Example of a Timepix data frame. This is one of the MiniPIX data frames from the 2019 mission.

fit line can be seen in Figure 11. L can now be calculated using L_p and T , the thickness of the sensor,

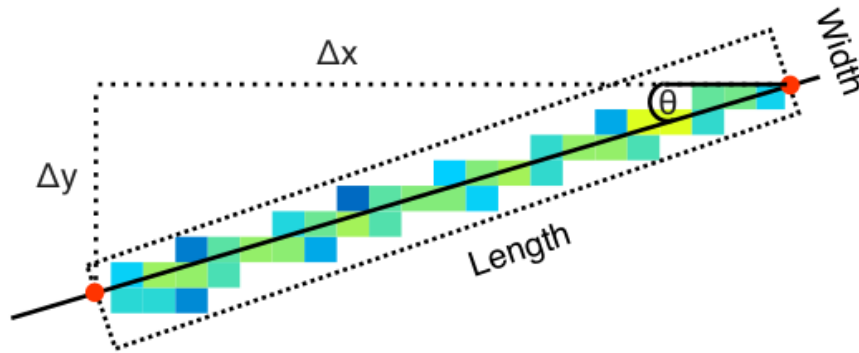


FIG. 11. A visual from Ref. [32] which shows the minimum-area bounding box (the dotted black box surrounding the particle track) and the linear least square fit line (the solid black line running along the particle track).

with

$$L = \sqrt{L_p^2 + T^2}.$$

Since T is a known property of the sensor, the LET value can then be calculated on a per particle basis. While out of the scope of the SORA 3 studies, the LET can be used to calculate the dose equivalent in human flesh.

The primary method of categorizing the particle incident on the detector is by the morphology of the resulting cluster. The track seen in the detector data will change its shape depending on the energy and the type of the particle. The actual identity of the incident particle cannot be directly measured by the sensor, but an inference can be made by using the energy and shape of the cluster. Ref. [32] gives some examples, stating that heavy tracks often correspond to high energy protons and alpha particles, medium blobs can correspond to very slow charged particles, straight tracks can be caused by light minimum ionizing particles (e.g. muon, pion). and light tracks can be caused by electrons and positrons. Figure 12 shows the classifications used in the SORA experiments.


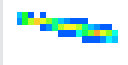


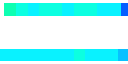

Type	Inner Pixels	Length/ Width Ratio	Other Criteria	Example Tracks
Small Blob	0	-	1 or 2 Pixels, 3 if L shape, 4 is square	
Heavy Track	> 4	> 1.25	Not S.Blob Density > 0.3	
Heavy Blob	> 4	< 1.25	Not H.Track Density > 0.5	
Medium Blob	> 1	< 1.25	Not H.Blob Density > 0.5	
Straight Track	0	> 8	Not M.Blob Minor axis < 3 pixels	
Light Track	-	-	Not S.Track	

FIG. 12. A visual from Ref. [32] showing the categories of tracks. This classification system is the same that is used in the SORA experiments.

3.3. Organic Solar Cell Methods

3.3.1. Fabrication

We began by developing the fabrication procedure for each layer in the stack. To achieve thin films from liquid solutions we use spin coating is for the EBL, ETL, and active layer. The liquid solution is deposited onto the surface of a substrate that is spun at a high RPM, flinging the solution out to the edges through centripetal forces and resulting a thin, ideally uniform, layer. After spinning the substrate is moved into the a hot plate where any remaining solvent is evaporated and a solid thin film remains. The top electrode is deposited by means of sputter coating. FTO slides, 0.5-1% PEDOT:PSS in H₂O solution, and platinum sources were all used as purchased from suppliers without further modification.

The EBL titania layer was synthesized through a sol gel process resulting in an amorphous phase, which when applied during spin coating and further annealed creates a dense noncrystalline layer. The sol gel titania solution was provided by Lilly Schaffer and prepared prior to our arrival at the lab. Titania was held

in the fridge when not in use.

The active layer was prepared in a 1:1 ratio between P3HT and PCBM[24] 12.5 mg of P3HT was diluted in 0.5 mL of chlorobenzene (CB) and 12.5 mg of PCBM was also diluted in 0.5 mL of CB. Both solutions were ultra sonicated before being combined into one solution and further sonicated to ensure an even mixing of P3HT and PCBM. We attempted to use a small magnetic stir bar to agitate and mix the solution but this proved ineffective due to the small size of the stir bar and the height of the vessel containing our solution. Any active layer solution not immediately used is held in the desiccator.

We will outline our typical fabrication process below without detailing any specific run:

FTO slides are first cleaned with a chemical soap scrub and then with a deionized water, isopropanol, and acetone ultrasonic bath successively before being dried under nitrogen and heated in the oven at 150 °C for an hour. Clean slides were then taken to the spin coater for application of the titania EBL. The entire slide is loaded onto the spin coater and covered completely in the titania. We then spun at 2000 rpm for 20 seconds to achieve a uniform hazy film. Each slide was then taken to the oven to anneal at 550 °C for 30 minutes, then a second titania layer is deposited in the same method. Immediately following the film application a chemwipe or razorblade was used to remove a portion of the film from one side and expose the FTO. Cells were then left to anneal at 550 °C for 5 hours, then cool to room temperature.

After annealing the slides were taken back to the spin coater. 75 μ L of active solution was deposited at 100 RPM for 5 seconds before ramping up to 1000 RPM for 25 seconds. Each slide was set on a hot plate at 150 °C for 10 minutes before returning to the spin coater. 200 μ L PEDOT:PSS was deposited by drop casting before spin coating at 500 RPM for 5 seconds then ramped up to 5000 RPM for 25 seconds. Slides were then returned to the hot plate for 10 minutes. Each slide was then covered by a mask and set into the Leica EM SDC050 sputter coater that was loaded with a platinum source before being brought to a vacuum level ($<10 \times 10^{-2}$ mbar). The high voltage was then turned on and allowed to sputter for 150 seconds.

4. RESULTS

The SORA 3 payload recorded a total of 13859 data packets during flight. The approximately 15 minutes long gap seen in all data plots is due to the down time that the HASP administration ordered in response to the faulty battery sensor. Fortunately, this gap in data did not cause any issues. One important incident to note that occurred midflight was the overheating of the MiniPIX device. This issue occurred when the device reached about 90 °C at approximately 15:36:09 on September 5th. Once this happened, the MiniPIX shutdown and the payload halted functionality. The MiniPIX overheating was a direct result of the MiniPIX not having proper heat sinks. The MiniPIX was directly connected to the aluminum chassis of the ISS module to use as a heat sink, but this was not effective enough. Had the astrobiology system functioned properly, a power cycle command would have been sent to the payload, and the entire system would have successfully rebooted. Upon shutting down, the astrobiology system would have retracted, however, this would have potentially caused the lid of the astrobiology system to become detached from the payload thus creating a loose projectile that could have fallen off the balloon gondola. The team did not want to risk this happening, so the payload was not power cycled. This resulted in a lack of data collection for the remainder of flight.

All systems withstood the landing impact. The payload was returned to UH with no sustained damage, and every component was functional.

4.1. Astrobiology Results

The SORA astrobiology team is currently still waiting for the biological samples collected during the flight to be sequenced and analyzed by Dr. Preethi Gunaratne’s biochemical research laboratory at the University of Houston. Despite this lack of data, conclusions may still be drawn with respect to the success of this year’s mission. A typical DNA extraction kit was used to extract and purify the DNA found in both the control and experimental samples. The extraction separated the DNA in the samples from other biological molecules (proteins, lipids, etc.) of no interest, making the samples suitable for sequencing. All members of the astrobiology team participated in the extraction, under the supervision of Dr. Donna Pattison, a faculty member of the University of Houston Department of Biology and Biochemistry. The prepared samples were then sent to Dr. Gunaratne’s lab to await sequencing. The sequencing procedure will be very similar to those of the two previous missions, with some notable differences. In the sequencing of the samples obtained from the 2018 mission, it was found that the data was not consistent with that of the 2017 mission—most notably, there was an absence of archaea, a domain of life encompassing organisms that resemble bacteria and are known for their ability to survive in extreme conditions. However, after further investigation, it was found that improper primers were used in the 2018 analysis, making it very possible that data regarding archaea was lost. Primers, which amplify the signal of the DNA being analyzed to detectable levels, are very particular to the class of the organism being studied; thus, picking primers appropriate to the situation is vital. With this to consider, it has been assured that the Gunaratne lab will use primers that will apply to a broader range of organisms, including archaea. Despite the contamination of the samples, it is hoped that the data obtained will confirm some of our previous findings, and provide a better starting point for any future missions.

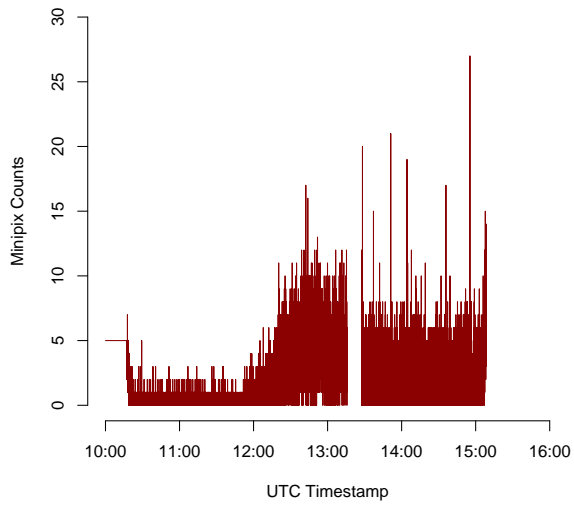
4.2. Cosmic Radiation Results

The FITPix recorded a total of 15810 frames, and the MiniPIX recorded a total of 15735 frames. Upon integration in the Fort Sumner hangar, the environmental used in the ISS module ceased to function. Prior to leaving the UH campus, the sensor was functioning and sending data to the Arduino MEGA. It is suspected that the sensor may have disconnected during transit from the UH campus to Fort Sumner. Due to this, the environment inside the ISS module was unknown during flight.

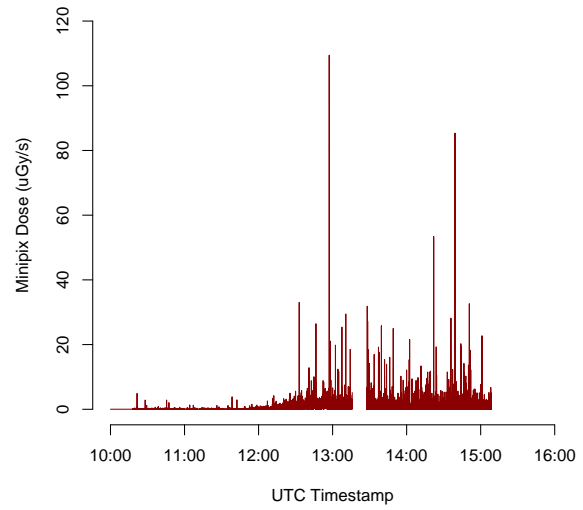
4.3. Organic Solar Cell Results

The main goal of the solar cell experiment was to observe changes in the structure and performance of the organic solar cells before and after being exposed to the stratosphere. The purpose of the current reading circuit for the solar cells was mainly to provide a proof-of-concept in order to show that it is possible to easily perform the IV measurements within the context of our payload. The current reading circuit that was flown accomplished this goal. The data recorded by the current reading circuit was legible enough to clearly see the relationship between current produced by the cell and the voltage applied across the cell. However, the data is not precise enough to determine values such as V_{oc} or I_{sc} . An IV curve that was measured using lab equipment is shown next to an example of data recorded by the current reading circuit in Figure 20. Due to the variability of the data recorded by our circuit, it is not possible to use this data for any calculations. Only one plot is shown since all measurements made by the circuit look similar. A discussion of potential improvements for this circuit can be found in Section 5.1.

Although we experienced difficulties during our mission, we believe that continued investigation into the use of organic semiconductors for space applications is needed. We believe a more thorough and detailed investigation is needed to truly understand the operation of OPVs in the stratosphere. Ideally a dedicated long term launch with on board spectrometers and potentiostats to precisely determine in situ properties across a variety of OPV varieties would be conducted. A detailed investigation like this would include extensive characterization beyond JV curves, such as photoluminescence, electroluminescence, reflectivity, capacitance-voltage, capacitance-frequency, and external quantum efficiency. Continued additional missions

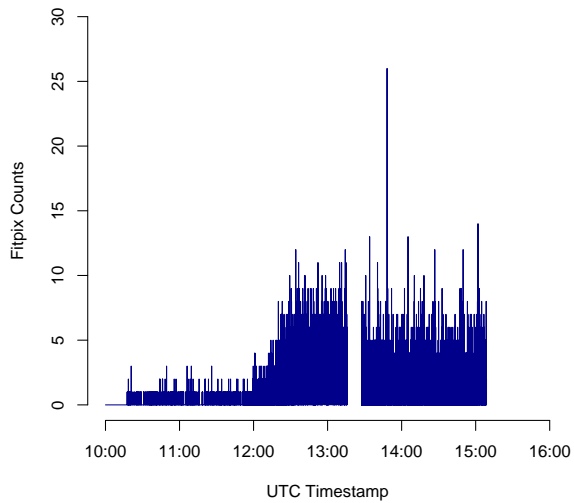


(a) MiniPIX counts measured during the 2019 flight.

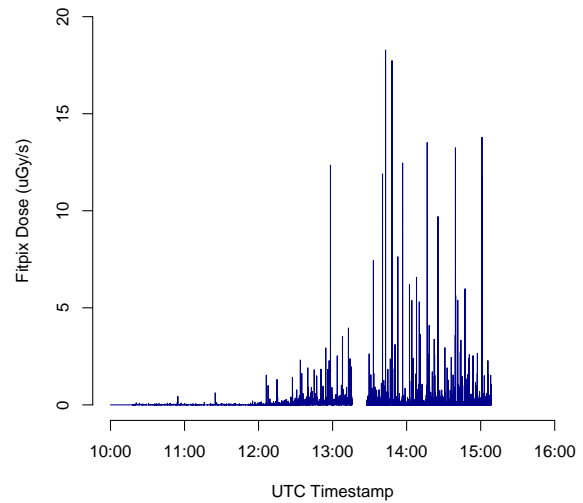


(b) MiniPIX dose measured during the 2019 flight.

FIG. 13. MiniPIX particle data recorded during the 2019 flight.



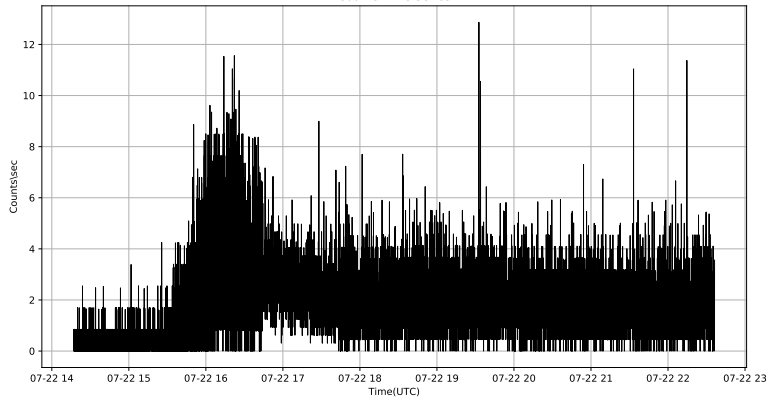
(a) FITPix counts measured during the 2019 flight.



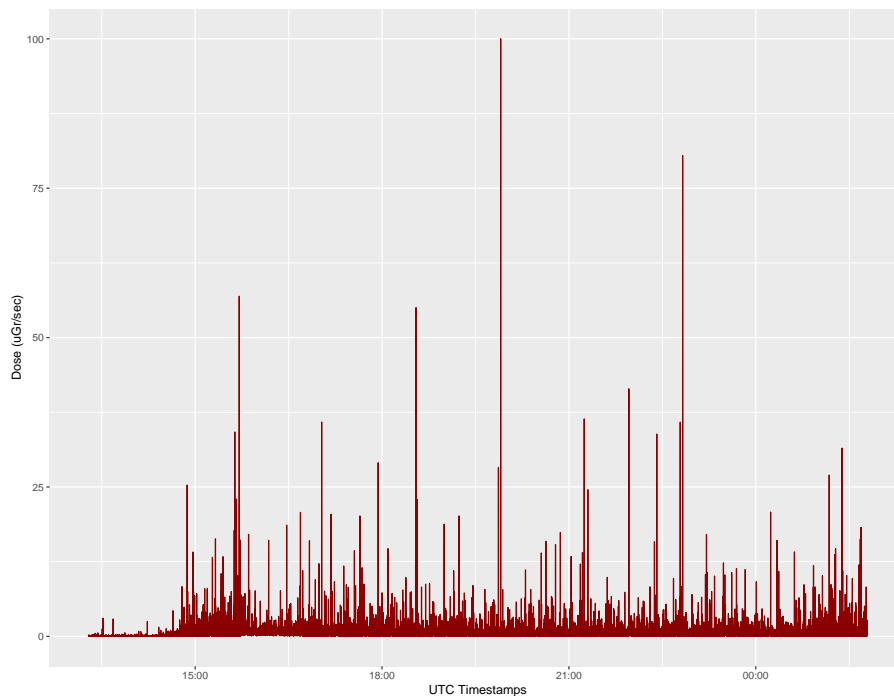
(b) FITPix dose measure during the 2019 flight.

FIG. 14. FITPix particle data recorded during the 2019 flight.

can also be useful to understand how the space environment can effect the morphology of cells, particularly in the highly performing perovskite based solar cells.



(a) MiniPIX counts measured during the 2018 flight.



(b) MiniPIX dose measured during the 2018 flight.

FIG. 15. MiniPIX particle data recorded during the 2018 flight.

5. DISCUSSION

By the terms of success defined at the beginning of the mission, the SORA 3 payload did not succeed in its goals. The payload faced difficulties in each of its subexperiments for varying reasons, however, each experiment did have varying ranges of success, which will be discussed in the subsequent sections. Despite the failures, the payload was designed and constructed well, and only minor improvements to certain aspects of the payload would be necessary to fix the payload as a whole.

One important improvement to the payload would be to add more specialized commands to the list of available commands. For example, separate commands could be used to rotate the astrobiology arm clockwise by 1° , rotate the arm clockwise by 5° , rotate the arm clockwise by 15° , rotate the arm clockwise by 45° , and similar commands corresponding to the counter-clockwise direction. Other commands could be to reboot one particular radiation device at a time as opposed to rebooting the entire system. Of course, in an ideal situation, the use of such commands would not be necessary. Another important and necessary improvement

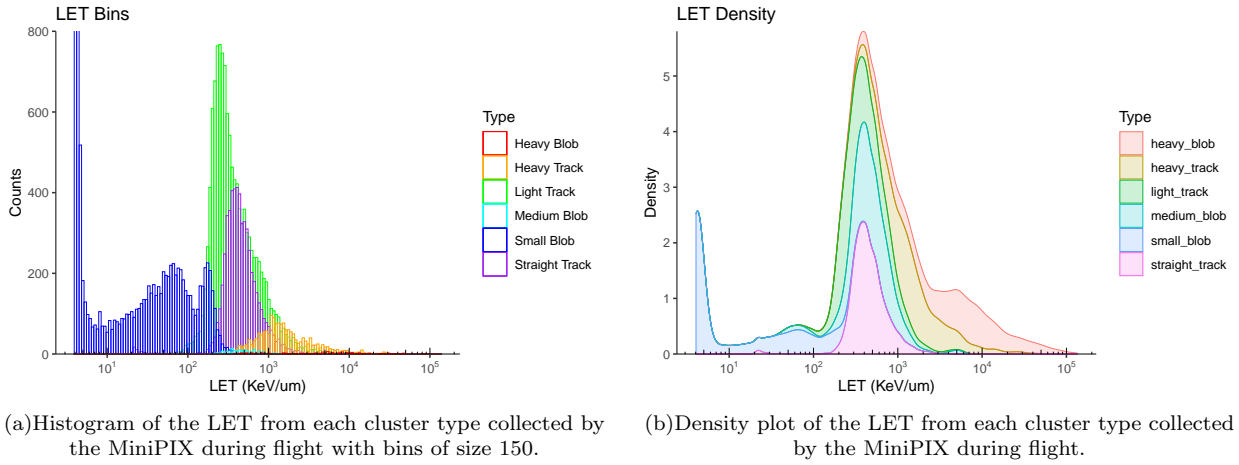


FIG. 16. MiniPIX LET distributions from flight data.

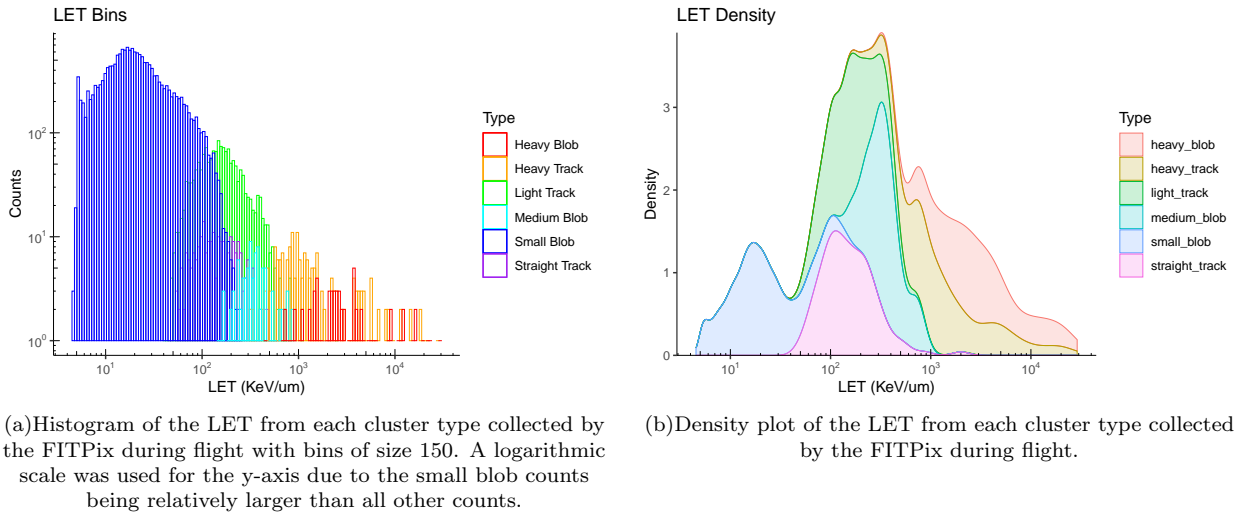


FIG. 17. FITPix LET distributions from flight data.

to the payload would be to add a larger heatsink to the inside of the ISS module, which would prevent the MiniPIX from overheating. This can easily be done with a large block of aluminum similar to the one used in the FITPix container.

5.1. Electronics Discussion

We opted to use a current to voltage converter, also known as a transimpedance amplifier, in order to collect data necessary to characterize the organic solar cells. This was used primarily because it is a relatively simple circuit which was already known of that would not add any additional resistance in the solar cell's current path, thus not reducing the current through the cell. The preferred method would be to utilize a proper current shunt monitor integrated circuit (IC) in a high-side sensing arrangement. This would allow for more responsiveness to measuring current flowing through the solar cell. The method of a shunt monitor works by measuring the current through a shunt resistor. Since the shunt monitor is comprised of a match differential amplifier with high input impedance the shunt resistance seen by the solar cell would be practically zero and would also not alter the current flowing through the cell.

To collect readings of the voltages produced from the solar cell currents we opted to use the Arduino

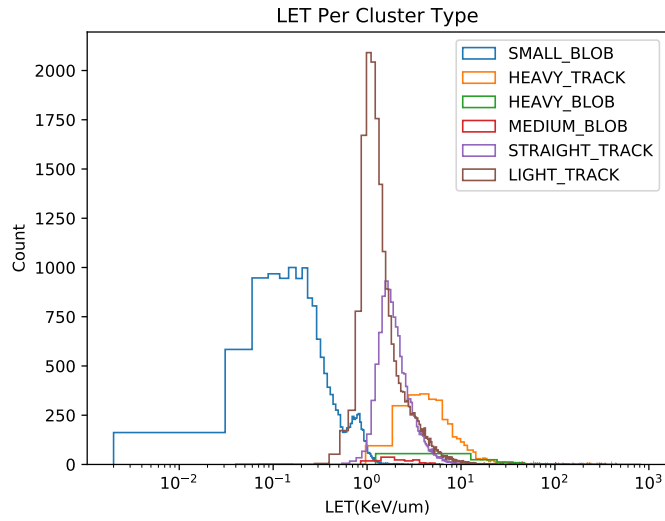


FIG. 18. Histogram of the LET spectrum for the 2018 mission.

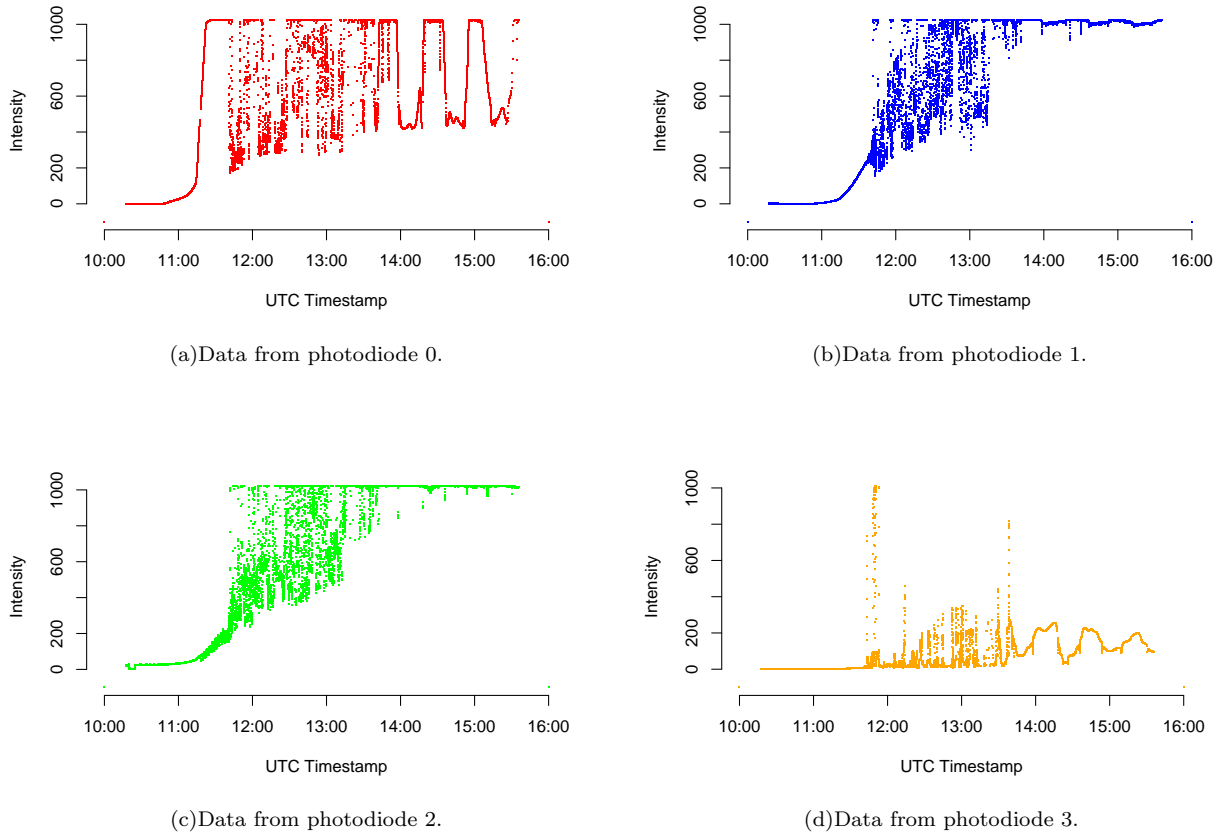
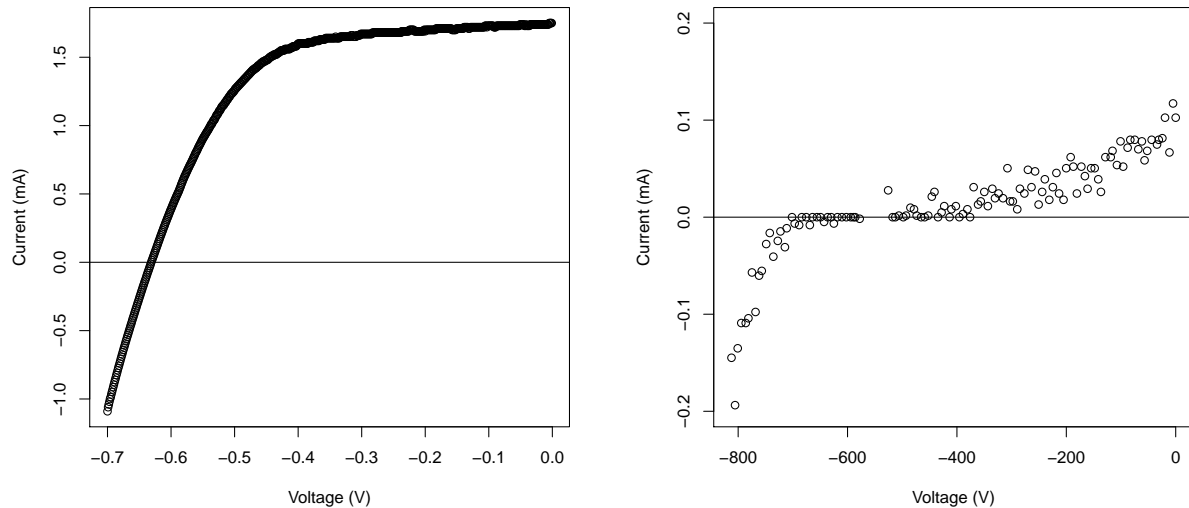


FIG. 19. Photodiode data from the flight.

MEGA `anaLogRead()` capability which is able to read voltages up to 5 V. It is not recommended to read negative voltages, but since we were reading voltages with very small currents the Arduino was not in danger



(a) IV curve recorded by the equipment in the solar cell fabrication lab. This plot was made immediately after fabricating the cell. There had not been enough time for the cell to degrade which is why this plot is so well-defined.

(b) IV curve recorded by SORA 3's IV measuring circuit. This plot was made a considerable time after the cell was fabricated, which is why it is not very well-defined.

FIG. 20. IV curves measured by two different sources.

of being damaged. The issue with using an Arduino MEGA is that it has an analog to digital converter (ADC) resolution of 10 bits at a maximum voltage reading of 5 V which equates to an error of ± 4.89 mV. There is the Arduino Due which is capable of 12-bit ADC resolution which would equate to an error of ± 1.22 mV and would give a 25% greater precision of data collection. There are 16-bit ADC's available as packaged IC's but they can be cost prohibitive especially when collecting data from a large array of solar cells. One improvement that could be made in addition to choosing a higher bit microcontroller or IC is the use of a digipot with a higher step count. The digipot used in the SORA 3 payload had 128 steps since a higher step digipot would be useless with our 10-bit Arduino MEGA. Some digipots can have as many as 1024 steps, which would allow a voltage sweep from 0 V to 0.8 V with a resolution of 0.78 mV. This resolution would be as high as the equipment used to test the solar cells in the lab.

The biggest downfall of our constructed circuit is that there is a wide range of voltage values surrounding V_{oc} at which the circuit measures zero current. The current at those values is on the order of nanoamperes, which is well below the resolution of our circuit. Simultaneously being bale to read current on the order of nanoamps as well as microamps would prove to be quite a technical challenge, but such an endeavor would certainly be worthwhile for future experiments.

5.2. Astrobiology Discussion

During the flight, the astrobiology collection system experienced mechanical difficulties that greatly damaged the integrity of the samples collected. The cameras on the payload showed that, while the collection system had successfully deployed, the rotating collection arms had stopped mid-turn. This situation, while not ideal, would have still proven workable if not for the fact that this also meant that the lid of the collection system was unable to close, leaving the stratospheric samples exposed to contamination. All attempts to resume the rotation of the system were unsuccessful, and while the option of attempting to close the box was considered it was ultimately decided that the risk of the lid popping off and becoming a dangerous projectile was too high. Thus, the collection system box was open and exposed during descent and landing, and remained so until the box was retrieved. Despite the compromised state of the samples, it was decided that the samples would still be sequenced to see if any useful data could be obtained to inform future missions.

This error could be solved with a circular design for the lid as that would prevent the lid from not being able to close properly.

5.3. Radiation Discussion

5.3.1. Cosmic Radiation

As can be seen by comparing Figures 13(a) and 14(a), the MiniPIX and FITPix recorded a similar number of counts throughout the duration of flight despite the differing energy thresholds for the devices. Both the trend and values of the 2019 counts almost exactly match that of the 2018 SORA mission, which is shown in Figure 15(a). The MiniPIX and FITPix dose measurements are slightly different in value due to the difference in energy threshold between the two detectors, but the plots follow the same trend. Interestingly, the 2019 MiniPIX data has a small but noticeably higher average dose than the 2018 MiniPIX data. The average dose rate for the 2019 data is $0.578 \mu\text{Gy/s}$ while the average dose rate over the same period of time for the 2018 MiniPIX data is $0.499 \mu\text{Gy/s}$. There is a 15.8% increase from 2018 to 2019. While this is not a substantial increase, this increase can likely be attributed to the change in the device's environment. Further investigation through future experiments is certainly needed in order to make a definitive claim.

The MiniPIX LET histogram possesses a remarkably similar shape to the LET histogram of the 2018 mission data, which can be seen in Figure 18. The primary difference between the two data sets is the total counts, which is understandable considering the 2018 mission had a longer duration than the 2019 mission. The density plots for both the MiniPIX and the FITPix LET spectra clearly show that the majority of LET values lie within the $100 \text{ keV}/\mu\text{m}$ to $1000 \text{ keV}/\mu\text{m}$ range.

Further investigations into the effectiveness of the ISS module would certainly be worthwhile. As previously mentioned, developing an accurate and low-cost radiation dosimeter is of increasing importance with the increasing presence of humans in space. While computational models are a powerful tool, they are currently not well-suited for monitoring the well being of astronauts and their exposure to radiation. Schwadron et. al. [33] from the CRaTER experiment found that the observed dose rates in the interplanetary environment exceed computational predictions by about 10%.

Understanding and monitoring thermal neutrons is important for the safety of astronauts and airline passengers. This idea was mentioned in the 2018 SORA mission report, which attempted to monitor neutrons with the use of a scintillator. The scintillator used in that experiment did not yield any results, so further investigations into determining an effective scintillating material to use with a Timepix device is worthwhile. Furthermore, monitoring the solar cycle with a Timpix dosimeter would be an interesting application and a good testbed of such a device. Hathaway has shown a direct relationship between the average neutron counts and the development of the solar cycle [11].

5.3.2. Organic Solar Cells

With no prior experience in fabrication of organic semiconductors, the OPV program proved to be a greater, but rewarding, challenge than predicted. The radiation group gained indispensable experience in theoretical and experimental techniques of organic photovoltaics, ranging from the basic properties of conjugated polymers to synthesis of sol-gels and current-voltage profiling. Beyond the fundamental work with OPVs, we also considered the energy demands for future space missions. With the rapid rise of private space launch companies and the plans for trips to mars and beyond, lightweight and flexible solar panels with high specific power are most desirable to be developed. In situ manufacturability is one of the great advantages that OPVs offer to the space energy environment, where roll-to-roll processing can be conducted easily[23]. A few days prior to the team's departure to New Mexico, several difficulties cropped up regarding the organic solar cell fabrication. The fabrication lab was experiencing issues with the quality of the materials, and the cells that were produced could not meet the usual efficiencies of cells produced in the lab. Furthermore, the current-reading circuit could not perform as intended. The circuit itself was properly

designed to account for the 24 cells that were originally planned to be used, but there was an incompatibility between the multiplexers and the operational amplifiers used in the circuit. As a result of both the cell fabrication difficulties and the circuit incompatibility, the number of cells was reduced. The current reading circuit was connected directly to the Arduino MEGA since the multiplexers needed to be removed. Three cells were used for flight since the Arduino MEGA could only accommodate six direct connections to its analog pins (two connections per cell). The reason for this incompatibility is still unknown, but it likely has to do with the internals of the chips.

6. CONCLUSION

Overall, the SORA 3 payload did not succeed. The SORA 3 experiment received a major overhaul in comparison to the previous two iterations of SORA, and this resulted in some new issues that arose during flight. The astrobiology experiment failed due to deformation in the lid of the astrobiology box. The tight tolerance between the bottom of the filter flaps and the top rim of the clean box resulted in the lid getting stuck on the side of the box, and the experiment to not function properly. Had this gap been a couple of millimeters larger, this issue would not have occurred, and the astrobiology box lid would have been able to rotate freely. The failure of the astrobiology experiment had a snowball effect, which resulted in an overall shutdown of the payload. The MiniPIX device overheated, and this resulted in a halt of data collection for the entire payload. If the astrobiology system was functioning properly, the payload could have been rebooted in order to restart the data collection system, and the payload could have functioned normally.

Despite the issues faced during the SORA 3 experiment, the MiniPIX and FITPix devices were able to return meaningful data that can be compared to previous and future radiation dosimetry flights. Additionally, the methodology tried by the SORA 3 payload has resulted in a wealth of knowledge for future attempts. Slight improvements can be made to the astrobiology and radiation systems to ensure proper and continued functionality of the systems for the duration of a typical balloon flight. Furthermore, the introduction of the organic solar cell experiment led to a clear definition of what works for a solar cell experiment in this context.

Most importantly, the SORA 3 experiment offered real-world, hands-on experience to over a dozen undergraduate students. Every participant gained in-depth knowledge in their particular fields of interest and had the opportunity to make a contribution to a project that lies within that field. Had the team been given the opportunity to continue this work, the next iteration of the SORA experiment would have been able to utilize the information gained through the trials of the SORA 3 experiment and huge improvements could have been made.

Appendix A COLLABORATION DEMOGRAPHICAL INFORMATION

Name	Role	Student Status	Race	Ethnicity	Gender	Disabled
Andrew L. Renshaw	Faculty Mentor	Faculty	White	Non-Hispanic	Male	No
Reed Masek	Project Leader	Undergraduate	White	Non-Hispanic	Male	No
Jimish Patel	Astrobiology Coordinator	Undergraduate	Asian	Non-Hispanic	Male	No
Taylor Hill	Radiation Coordinator	Graduate Student	White	Non-Hispanic	Male	No
Daniel Howard	Electronics Coordinator	Undergraduate	White	Non-Hispanic	Male	No
Jose Alvarado	Organic Solar Cells	Undergraduate	White	Hispanic	Male	No
Carlos Amaya	Programming and Data Handling	Undergraduate	White	Hispanic	Male	No
Aaron Boggs	Organic Solar Cells	Undergraduate	White	Non-Hispanic	Male	No
Carson Bush	Astrobiology Planning and Construction	Undergraduate	White	Non-Hispanic	Female	No
Alejandro Carpy	Organic Solar Cells	Undergraduate	White	Hispanic	Male	No
Kevin Fleming	Astrobiology Construction	Undergraduate	White	Non-Hispanic	Male	No
Sydney Giang	Mechanical Engineering and Construction	Undergraduate	Asian	Non-Hispanic	Female	No
Emily Humble	Programming and Mechanical Control	Undergraduate	White	Non-Hispanic	Female	No
Khoa Ngo	Astrobiology Construction	Undergraduate	Asian	Non-Hispanic	Male	No
Huy Truong	Mechanical Engineering and Construction	Undergraduate	Asian	Non-Hispanic	Male	No
Abraham Vega	Mechanical Design	Undergraduate	White	Hispanic	Male	No
Stuart George	MiniPIX Expert	Post-Graduate	White	Non-Hispanic	Male	No
Donna Pattison	Faculty Mentor, Microbiology	Faculty	White	Non-Hispanic	Female	No
Preethi Gunaratne	Faculty Advisor	Faculty	Asian	Non-Hispanic	Female	No

Appendix B OUTREACH AND PUBLICATIONS

As requested by the HASP administration, this section details the relevant outreach and publications by those who are or have been in the University of Houston HASP team.

Some presentations do not have associated hyperlinks since the presentation was relatively informal and not for an official conference.

Outreach and Presentations:

1. Steven Oliver, UH Undergraduate Research Day, October 12, 2017, URL no longer available.
2. Samuel Morales, Bulletin of the American Physical Society, October 20, 2017, <https://meetings.aps.org/Meeting/TSF17/Session/E5.3>.
3. Fre'Etta Brooks, Rice University, APS Conferences for Undergraduate Women in Physics (CUiP), January 14, 2017, http://cuwip.rice.edu/cuwip_poster_session.html#poster15.
4. Steven Oliver, Andrew Walker, Kevin Portillo, and Reed Masek, Tarleton APS Conference Poster Presentation <http://meetings.aps.org/Meeting/TSS18/Session/D1.5>.
5. Steven Oliver, Presentation at University of Houston STEM Center's STEM Saturday, October 13, 2018.
6. Taylor Hill, Presentation at Mars Rover Celebration Award Ceremony, March 23, 2019.
7. Reed Masek, Presentation for NASA's Aerospace Scholars, July 8, 2019.

As of writing this report, there has been one publication conceived as a result of the HASP missions. The publication is in the end stages of writing, and will soon be sent to be reviewed by the publisher. The bibliography entry is as follows:

(In Progress) S.A. Garcia Morelos, A. Walker, R. B. Masek, S. Oliver, F. Brooks, K.D. Portillo, J. Patel, D. Pattison, A. L. Renshaw *MiniPIX Cosmic Ray Tracking and Radiation Dosimetry During SORA Stratospheric Balloon Flights*.

Appendix C INTERNSHIPS, JOBS, RECENT GRADUATES, AND GRADUATE SCHOOL

This section lists the internships and jobs received by participants in the UH HASP team.

The following is all of the HASP members who have received internships, the company or institution, the location, and the year of the internship.

Internships:

1. Kevin Portillo, Boeing Internship, Houston, Texas, 2018
2. Reed Masek, DAAD RISE Internship, Karlsruhe, Germany, 2018
3. Steven Oliver, NASA Johnson Space Center, Houston, Texas, 2019

The following is all of the HASP members who are working in industry, their company, their position, and the year they began.

Jobs:

1. Andrew Walker, NOV, Software Engineer, 2018
2. Andrew Walker, Gene by Gene, Software Engineer, 2019
3. Kevin Portillo, Chevron, Software Engineer, 2019

The following is all of the HASP members who have graduated within the past year, their degree, and when they graduated.

Recent Graduates:

1. Kevin Portillo, B.S. Computer Science, December 2018.
2. Taylor Hill, B.S. Physics, May 2019.
3. Jimish Patel, B.S. Physics, December 2019.
4. Daniel Howard, B.S. Electrical Engineering, December 2019.

The following is all of the HASP members who are enrolled in graduate studies, the institution, program, and the year they began.

Graduate School:

1. Steven Oliver, Rice University, Space Studies Masters Program, 2017
2. Fre'Etta Brooks, MD Anderson UT Health, Medical Physics Ph.D. Program, 2019

3. Taylor Hill, Colorado State University, Masters in Materials Sciences Engineering, 2019

The following are messages from previous HASP participants making personal comments on their successes after HASP and the experiences they had as part of the HASP program:

“This month (December 2019) I will be graduating from Rice University with a Professions Science Master’s Degree in Space Studies with a focus in engineering. I’m currently interning with Airbus Defence and Space (Space Systems, Inc.) as a Mechanical Design Engineer. I’m working on the design of the ArgUS multi-payload adapter mechanism for Bartolomeo external platform on the ISS. I also received a summer 2019 internship with the Space Radiation Analysis Group (SRAG) at NASA JSC as a research intern. My project focused on the validation of an existing Monte Carlo tool for the simulation of a Timepix (cosmic radiation detector) data to various ion beam measurements. I would like to thank the HASP program for allowing me to participate in the HASP 2017 and 2018 flights. My career path, education, and accomplishments prior mentioned directly stem from the experiences and skills I have gained from participating in the HASP flight program.”

-Steven Oliver

“Soon after graduating from the University of Houston with a B.S Computer Science degree, I began working as a Software Engineer at Chevron in Houston. Specifically, I work within embedded IT for Chevron’s Pipeline and Power’s Business Unit where we operate and manage the transportation of product from Upstream to Downstream as well as the cogeneration and renewable energy assets for all of Chevron. My role involves developing, supporting, and migrating applications used by my business unit. Our partnership with Microsoft allows me to develop, build, and deploy modern applications all through the cloud.”

-Kevin Portillo

-
- [1] Extremophiles <http://www.nytimes.com/2013/02/07/science/living-bacteria-found-deep-under-antarctic-ice-scientists-say.html>.
- [2] S. A. Garcia Morelos, F. Brooks, S. Oliver, A. Walker, K. D. Portillo, R. B. Masek, D. Mroczek, D. Pena, J. Juarez, A. Cruz, D. Henandez, S. George, D. Pattison, A. L. Renshaw. *SORA 2017 Mission Webpage*, <http://laspace.lsu.edu/hasp/groups/Payload.php?py=2017&pn=10>.
- [3] Christner, B., Alleman, M., Bryan, N., Burke, S., Guzik, T.G., Granger, D., King, G. (2013) *LSU HASP2013 PDF. Baton Rouge: Louisiana Space Consortium*.
- [4] Canales D. C. and Ehteshami A., *An attempt to sample atmospheric bacteria*, Houston, TX, 2015, January 11.
- [5] S. A. Garcia Morelos, F. Brooks, S. Oliver, A. Walker, K. D. Portillo, R. B. Masek, S. George, D. Pattison, A. L. Renshaw. *SORA 2 2018 Mission Webpage* <https://laspace.lsu.edu/hasp/groups/Payload.php?py=2018&pn=12>.
- [6] M. Lemoine and G. Sigl, "Physics and astrophysics of ultra-high-energy cosmic rays," in *Physics and Astrophysics of Ultra-High-Energy Cosmic Rays*, Lecture notes in physics, 576., (Berlin ;), Springer, 2001.
- [7] <https://home.cern/science/physics/cosmic-rays-particles-outer-space>
- [8] Schröder, F. G. (2017). Radio detection of cosmic-ray air showers and high-energy neutrinos. *Progress in Particle and Nuclear Physics*, 93, 1-68. doi:10.1016/j.pnpnp.2016.12.002
- [9] Regener E. and Pfozter G., *Vertical Intensity of Cosmic Rays by Threefold Coincidences in the Stratosphere.*, *Nature* 136, 718-719, (1935).
- [10] Sarkar, R., Chakrabarti, S., Pal, P., Bhowmick, D., and Bhattacharya, A. Measurement of secondary cosmic ray intensity at Regener-Pfozter height using low-cost weather balloons and its correlation with solar activity. *Advances in Space Research*, 60(5), 991-998. (2017). <https://doi.org/10.1016/j.asr.2017.05.014>.
- [11] Hathaway, D. The Solar Cycle. *Living Reviews in Solar Physics*, 7(1), 1-65. (2010). <https://doi.org/10.12942/lrsp-2010-1>.
- [12] U. Torterpun, D. Ruffolo, and J. W. Bieber, "Galactic Cosmic-Ray Anisotropy During the Forbush Decrease Starting 2013 April 13," *The Astrophysical Journal*, 852, (2018).
- [13] C. W. Lloyd, S. K. Townsend, and K. K. Reeves. *Space Radiation*. NASA, n.d.
- [14] N. A. Schwadron, J. B. Blake, A. W. Case, C. J. Joyce, et al., Does the worsening galactic cosmic radiation environment observed by CRaTER preclude future manned deep space exploration? *Space Weather*, 12, 622 - 632. (2014).
- [15] Medipix Collaboration at <https://medipix.web.cern.ch/>.
- [16] MiniPIX - Miniaturized Portable USB Photon Counting Camera. (n.d.). <http://advacam.com/camera/minipix>.
- [17] V Kraus et al. Fitpix Fast Interface for Timepix Pixel Detectors. *Journal of Instrumentation*, 6(01), C01079-C01079. (2011). <https://doi.org/10.1088/1748-0221/6/01/C01079>
- [18] Timepix chip at <https://medipix.web.cern.ch/technology-chip/timepix3-chip>
- [19] J Jakubek. Semiconductor Pixel Detectors and Their Applications in Life Sciences. *Journal of Instrumentation*, 4(03), P03013-P03013. (2009). <https://doi.org/10.1088/1748-0221/4/03/P03013>.
- [20] "Solar Power Technologies for Future Planetary Science Missions." NASA, NASA, <https://solarsystem.nasa.gov/resources/548/solar-power-technologies-for-future-planetary-science-missions/>.
- [21] Bailey, S.g., et al. "Thin-Film Organic-Based Solar Cells for Space Power." IECEC '02. 2002 37th Intersociety Energy Conversion Engineering Conference, 2002., doi:10.1109/iecec.2002.1392006.
- [22] Oku, Takeo, et al. "Fabrication and Characterization of CH₃NH₃PbI₃ Perovskite Solar Cells Added with Polysilanes." *International Journal of Photoenergy*, vol. 2018, 2018, pp. 1-7., doi:10.1155/2018/8654963.
- [23] "Fabrication of Flexible Polymer Solar Cells Roll-to-Roll." *AccessScience*, doi:10.1036/1097-8542.yb130129.
- [24] Kesinro, R. O., et al. "Fabrication of P3HT: PCBM Bulk Heterojunction Organic Solar Cell." *IOP Conference Series: Earth and Environmental Science*, vol. 331, 2019, p. 012028., doi:10.1088/1755-1315/331/1/012028.
- [25] Baek, Woon-Hyuk, et al. "Use of Fluorine-Doped Tin Oxide Instead of Indium Tin Oxide in Highly Efficient Air-Fabricated Inverted Polymer Solar Cells." *Applied Physics Letters*, vol. 96, no. 13, 2010, p. 133506., doi:10.1063/1.3374406.
- [26] Huang, Hui, and Wei Deng. "Introduction to Organic Solar Cells." *Organic and Hybrid Solar Cells*, 2014, pp. 1-18., doi:10.1007/978-3-319-10855-1_1.
- [27] Yoshikawa, Osamu, et al. "Enhanced Efficiency and Stability in P3HT:PCBM Bulk Heterojunction Solar Cell by Using TiO₂ Hole Blocking Layer." *MRS Proceedings*, vol. 965, 2006, doi:10.1557/proc-0965-s11-04.
- [28] <https://resources.winsystems.com/datasheets/ppm-dc-atx-p-ds.pdf>
- [29] <https://www.airspayce.com/mikem/arduino/AccelStepper/>
- [30] Christiansen, E. L., Lear, D. M. (2012). *Micrometeoroid and Orbital Debris Environment & Hypervelocity Shields [PowerPoint slides]*. Retrieved from <https://ntrs.nasa.gov/archive/nasa/casi.ntrs.nasa.gov/20120002584.pdf>.
- [31] Jan Jakubek, *Precise energy calibration of pixel detector working in time-over-threshold mode* Institute of Ex-

perimental and Applied Physics, Czech Technical University in Prague, Czech Republic, 2011.

[32] George, S., *Dosimetric Applications of Hybrid Pixel Detectors*, University of Wollongong, Australia, 2015.

[33] N. A. Schwadron, F. Rahmanifard, J. Wilson, A. P. Jordan, H. E. Spence, C. J. Joyce, J. B. Blake, A. W. Case, W. de Wet, W. M. Farrell, J. C. Kasper, M. D. Looper, N. Lugaz, L. Mays, J. E. Mazur, J. Niehof, N. Petro, C. W. Smith, L. W. Townsend, R. Winslow, and C. Zeitlin, “Update on the worsening particle radiation environment observed by crater and implications for future human deep-space exploration,” *Space Weather*, vol. 16, no. 3, pp. 289–303, 2018.